ANALYSIS OF DRUG RESISTANCE OF HEPATOCELLULAR CARCINOMA (HCC) CELLS IN 3D MULTICELLULAR SPHEROID MODEL

ECE SARIYAR

Master's Thesis

Graduate School

Izmir University of Economics

Izmir

2021

ANALYSIS OF DRUG RESISTANCE OF HEPATOCELLULAR CARCINOMA (HCC) CELLS IN 3D MULTICELLULAR SPHEROID MODEL

ECE SARIYAR

A Thesis Submitted to
The Graduate School of Izmir University of Economics
Master's Program in Bioengineering

İzmir
2021

ABSTRACT

ANALYSIS OF DRUG RESISTANCE OF HEPATOCELLULAR CARCINOMA (HCC) CELLS IN 3D MULTICELLULAR SPHEROID MODEL

Sarıyar, Ece

Master's Program in Bioengineering

Advisor: Assoc. Prof. Zeynep Fırtına Karagonlar

July, 2021

Liver cancer is the fourth leading cause of cancer deaths and the sixth most common cancer globally. Only 10-15% of the patients are suitable for surgical resection. Hepatocellular carcinoma (HCC) demonstrates resistance to local regional therapies and chemotherapy which results in low survival rates. Sorafenib is a multikinase inhibitor for advanced stage patients. It only increases lifespan for three months and sorafenib resistance is developed in the majority of the patients. Regorafenib, a multikinase inhibitor, was found as an option after Sorafenib therapy. Although regorafenib increases the overall survival of patients who progress on sorafenib, there is limited knowledge about the efficacy of this drug. Our preliminary studies have shown that cells that develop sorafenib resistance *in vitro* also have increased regorafenib resistance. Therefore, diagnosis of new mechanisms that decrease sorafenib resistance and/or increase the regorafenib response of cells that develop sorafenib resistance is of great importance for advanced HCC patients who will receive these treatments. Three-dimensional (3D) cell culture mimics multidimensional properties of tumors and reflects cell morphology, proliferation and

drug resistance of tumors, thus leading to more meaningful results for drug studies. In this thesis, a 3D tumor spheroid model was developed by co-culturing liver cancer cells with hepatic stellate cells and macrophages using the hanging drop method. In this model, the effect of regorafenib treatment on parental and sorafenib resistant spheroids was investigated and the differences between the parental and the drug resistant group were revealed. The results of this thesis contribute to the development of 3D culture models that can mimic tumors in HCC and reveal important data on the effect of regorafenib treatment on sorafenib resistant tumors. This thesis was funded by TÜBİTAK (Project No: SBAG 118S542).

Keywords: Hepatocellular carcinoma, sorafenib, regorafenib, 3D cell culture, drug resistance, hanging drop method

ÖZET

HEPATOSELÜLER KARSİNOMA (HSK) HÜCRELERİNİN 3 BOYUTLU ÇOK HÜCRELİ SFEROİD MODELİNDE İLAÇ DİRENCİNİN ANALİZİ

Sarıyar, Ece

Biyomühendislik Yüksek Lisans Programı

Danışman: Doç. Dr. Zeynep Fırtına Karagonlar

Temmuz, 2021

Karaciğer kanseri dünya çapında en sık görülen dördüncü kanserdir ve kansere bağlı ölümlerde altıncı sırada yer almaktadır. Sadece %10-15'i cerrahi rezeksiyona uygundur. Hepatoselüler karsinoma (HSK), local tedavilere ve kemoterapiye karşı direnci arttırdığı için sağkalım oranı düşüktür. İleri evre hastalar için uygulanan Sorafenib bir multikinaz inhibitörüdür ve FDA tarafından 2007 yılında onaylanmıştır. Ancak bu tedavi hasta sağkalım süresini sadece 3 ay uzatıp sorafenib tedavisi gören hastaların çoğunda sorafenibe karşı direnç geliştirmektedir. Başka bir multikinaz inhibitörü olan Regorafenib, Sorafenibe alternatif tedavi olarak bulunmuştur. Regorafenib, sorafenib tedavisi gören hastaların genel sağkalımını artırsa da, bu ilacın etkinliği hakkında sınırlı bilgi vardır. Ön çalışmalarımız, *in vitro* sorafenib direnci geliştiren hücrelerin de regorafenib direncinin arttığını göstermiştir. Bu nedenle, ileri evre HSK hastaları için sorafenib direncini azaltan ve/veya sorafenib direnci gelişen hücrelerin, regorafenib yanıtını artıran yeni mekanizmaların teşhisi büyük önem taşımaktadır. İlaç çalışmaları için, üç boyutlu (3B) hücre kültürü, tümörün çok boyutlu özelliklerini taklit edip, hücre morfolojisini, çoğalmasını ve ilaç direncini daha iyi

yansıtmaktadır. Bu tez kapsamında karaciğer kanseri hücrelerini hepatik stellat hücreler ve makrofajlar ile beraber ko-kültür edilebildiği asılı damla yöntemi ile 3 boyutlu tümör sferoidleri oluşturulması amaçlanmıştır. Bu tezde elde edilen sonuçlar, HSK'daki tümörleri taklit edebilen 3 boyutlu kültür modellerinin geliştirilmesine katkıda bulunmuştur ve sorafenib dirençli tümörlerin regorafenib tedavisi hakkında yeni bilgiler açığa çıkartmıştır. Bu çalışma TÜBİTAK tarafından desteklenmiştir (Proje No: SBAG 118S542).

Anahtar kelimeler: Hepataselüler Karsinoma, sorafenib, regorafenib, ilaç direnci, 3B hücre kültürü, asılı damla yöntemi

ACKNOWLEDGEMENTS

First, I would like to thank my supervisor, Assoc. Prof. Zeynep Fırtına Karagonlar, who always supported me and taught me to never give up. Her expertise is magnificent in formulating the research questions and methodology. Her understanding feedback pushed me to improve myself and brought my studies to a higher level from beginning to end of this thesis.

I would also like to thank Izmir Biomedicine and Genome Center Erdal Lab. on Stem Cell and Organiod Technologies Research Group Leader Prof. Dr. Esra ERDAL for her valuable guidance throughout my studies who provided me with the tools that I needed to choose the right direction and successfully complete my thesis.

I also would like to thank IBG Optical Imaging Unit Responsible Melek ÜÇÜNCÜ and IBG Flow Cytometry and Cell Sorting Research Technician Gözde ALKAN YEŞİLYURT for their perspectives and friendships.

I would like to thank my labmates Bilge KARAÇIÇEK, Ceyda ÇALIŞKAN, Mustafa KARABİÇİCİ, Soheil AKBARİ, Nevin ERSOY, Berna BIÇAK, Melis KANIK and Alara TURGUT in Erdal Lab and Elifsu POLATLI, Sude UYULGAN in Güven Lab from Izmir Biomedicine and Genome Center. I would like to thank to my friends Hüseyin Saygın PORTAKAL, Arda KIPÇAK, Sıla Naz KÖSE in Izmir University of Economics. Lastly, I would like to thank to Ayşenur GÖNEN and Berat GÖKSEL from JCI Karşıyaka.

Special thanks to my dearest friends Bensu GÜNAY, Ezgi Ebrar ARABACI, Duygu GEÇKİN and Bilge CAN for encouraging and supporting me.

I would like to thank my lovely family, Safiye SARIYAR and İbrahim SARIYAR, who always believed and trusted me.

TABLE OF CONTENTS

LIST OF FIGURES

LIST OF ABBREVIATIONS

α-SMA: Alpha smooth muscle actin

ABC: ATP-binding casette

Abs: Array Buffers

AFP: Alpha-fetoprotein.

ATP: Adenosine triphosphate

BSA: Bovine serum albumin

CAFs: Cancer associated fibroblasts

Calcein AM: Calcein acetoxymethyl

CCL5: C-C motif chemokine ligand 5

CSCs: Cancer stem cells

DAPI: 4′,6-diamidino-2-phenylindole

DMEM: Dulbecco's Modified Eagle Medium

DMSO: Dimethyl sulfoxide

ECM: Extracellular matrix

EMT: Epithelial-mesenchymal transition

EGFR: Epidermal growth factor receptor

EpCAM: Epithelial cell adhesion molecule

FBS: Fetal Bovine Serum

FGFR: Fibroblast growth factor receptors

FSP-1: Peri-tumor fibroblast

HCC: Hepatocellular carcinoma

HGF: Hepatocyte growth factor

Hh: Hedgehog

HSCs: Hepatic stellate cells

IFN: Interferon

IL-: Interleukin-

LCSCs: Liver cancer stem cells

LPS: Lipopolysaccharide

MDR: Multidrug resistance

MDSCs: Myeloid-derived suppressor cells

MTT: 3-(4,5-dimethylthiazol-2-yl)-2,5-diphenyl tetrazolium bromide

NOS: Nitric oxide synthase

PBS: Phosphate-buffered saline

PEG: Polyethylene glycol

PES: Polyethersulfone

PD-L1: Programmed cell death ligand 1

PDGFR: platelet-derived growth factor receptor

PI: Propidium Iodide

PMA: Phorbol 12-myristate 13-acetate

Poly-HEMA: Poly (2-hydroxyethyl methacrylate)

RPMI 1640: Roswell Park Memorial Institute 1640

RT: Room temperature

STAT: Signal transducer and activator of transcription

SDS: Sodium dodecyl sulfate

TGF-β: Transforming growth factor-β

TAMs: Tumor-associated macrophages

TECs: Tumor endothelial cells

TME: Tumor microenvironment

TNFα: Tumor necrosis factor alpha

ULA: Ultra low attachment

VEGF: Vascular endothelial growth factor

VEGFR: Vascular endothelial growth factor receptor

Tie-2: Tyrosine-Protein Kinase Receptor 2

TECs: The tumor endothelial cells

CHAPTER 1: INTRODUCTION

Liver cancer is the fourth leading cause of cancer deaths and the sixth most common cancer globally (Whittaker, Marais and Zhu, 2010). Hepatocellular carcinoma (HCC), Cholangiocarcinoma, Liver angiosarcoma, and Hepatoblastoma are major types of primary liver cancer. Among all liver cancers, HCC is the most common type worldwide, with a rate of approximately 75%. Hepatitis infection (HBV or HCV), metabolic syndrome (obesity, diabetes) and toxins (alcohol) are important risk factors which influence HCC via triggering liver tissue damage leading to hepatic regeneration and cirrhosis (Wong et al., 2021). The treatment options include liver transplantation, transarterial chemoembolization, surgical resection and systemic chemotherapy for HCC patients. Although surgical resection is usually the first and most effective option, only 10-15% of the patients are suitable for this at the time of diagnosis (Jeong et al., 2017). Also, HCC patients develop resistance to systemic chemotherapy and local regional therapies. Moreover, conventional chemotherapy results in low survival rates. Sorafenib is the first multikinase inhibitor approved for advanced HCC patients and a current first-line treatment option applied worldwide to advanced stage HCC patients. However, Sorafenib only increases lifespan for 3 months and patients are reported to develop resistance (Llovet et al., 2008). Regorafenib, an analog of Sorafenib with a higher potency, was approved in 2017 to be used as a second-line treatment option after Sorafenib failure. Although regorafenib increases the overall survival of patients who progress on sorafenib, the efficacy of this drug is also limited by primary or acquired therapy resistance.

There are several crucial factors that contribute to poor drug response and high drug resistance of HCC such as activation of signaling pathways, complex interaction of HCC cells with tumor niche, induction of epithelial-mesenchymal transition (EMT) upon treatment, and high degree of genetic/ epigenetic dysregulation. These factors work together to assist HCC evolution and drug resistance (Villanueva et al., 2007). Recently, studies have shown that tumorigenicity of cancer cells is greatly affected by tumor microenvironment (TME) (R. Seo, 2015). TME is the cellular environment where the tumor tissue composition exists as extracellular matrix (ECM), immune cells, activated fibroblast, adipocytes, lymphatic endothelial cells, glial cells, pericytes, epithelial cells, signalling molecules, proteins and vascular cells (Siraj et al., 2019). The research in recent years indicated the importance of the tumor microenvironment

in HCC initiation, progression, and metastasis, obviously demonstrating that TME is an active component of the tumor. Not surprisingly, both Sorafenib and Regorafenib target signalling pathways important in tumor-stromal interactions and inflammatory pathways. Thereby, the interaction between TME and tumor cells is an important candidate for targeting heterogeneous features of HCC and identifying effective treatment strategies. However, there are no current cell culture models that can mimic HCC TME in the laboratory. The cell culture models that include TME would enable to study the effect of TME-HCC interaction on HCC drug response and resistance and would greatly contribute to developments in HCC prognosis and HCC treatment. Thus, it is important to improve a cell culture model that has the ability to mimic TME with multiple cell types.

In our study, we first aimed to develop a 3-D co-culture model using HCC cells (parental and sorafenib resistant), hepatic stellate cell line LX-2 and human monocyte cell line THP-1. Our model aims to mimic tumor microenvironment by growing parental and sorafenib resistant HCC cells in the presence of LX-2 and THP-1 cells. Moreover, we utilized hanging-drop technique in which these cells can be grown without adhering to cell culture plates in the form of tumor spheroids. In this 3-D co-culture model, we then aimed to characterize the differences between tumor spheroids established using parental and sorafenib resistant HCC cells. Our results demonstrate that sorafenib resistant tumor spheroids are different from parental tumor spheroids in cancer stem cell expression and regorafenib resistance. Moreover, there is a basal level of hepatic stellate cell activation and monocyte differentiation in sorafenib resistant tumor spheroids. Our findings reveal that drug resistant HCC cells interact differently with TME cells and co-culture models are crucial in order to identify target molecules that could be used to overcome therapy resistance.

CHAPTER 2: LITERATURE REVIEW

Hepatocytes and hepatic lobule, vascular system, hepatic sinsusoidal cells, biliary system and stroma are parts that form liver (Ishibashi and Nakamura, 2009). Hepatocytes are parenchymal cells which consist of 60% of the liver and they metabolize all the substances which are absorbed from the gut (Racanelli and Rehermann, 2006). Kupffer cells, stellate cells, endothelial cells and lymphocytes are non-parenchymal cells which highly contribute to liver function and homeostasis (Gao, Jeong and Tian, 2008).

HCC is the most common primary liver cancer with approximately 85 % rate. Chronic hepatitis caused by hepatitis B virus, hepatitis C virus and non-alcoholic steatohepatitis are risk factors to develop HCC (Birgani and Carloni, 2017). The majority of diagnosis is done at an advanced stage where HCC patients are not suitable for potentially curative therapies including liver transplantation or surgical resection. Therefore, systemic therapy still is the main therapeutic option for advanced HCC patients (Ohri et al., 2016).

Sorafenib is the first FDA approved multikinase inhibitor as a first line treatment for HCC patients. Sorafenib was approved in 2007 after SHARP trial, in which 602 patients, including 299 who were treated with sorafenib (800 mg/day) and 303 patients treated with placebo, took part. Results demonstrated that sorafenib improved survival rates and progression time of advanced HCC patients. (Llovet et al., 2008). Afterwards, another trial which is the Asia-Pacific trial also concluded more successful survival rates and progression time with sorafenib (Cheng et al., 2009).

A more recent trial, REFLECT trial (phase III study) showed the impact of lentavinib, which is also a multi kinase inhibitor that targets VEGFR1-3 and other kinases. Lentavinib is more attractive to the FGFR family especially VEGF receptors and it has encouraging efficiency in hepatitis B virus infected patients and high AFP level patients (Raoul et al., 2019). In addition to Lenvatinib, combination of programmed cell death ligand 1 (PD-L1) inhibitor atezolizumab and VEGFR inhibitor bevacizumab were also approved for first-line treatment for advanced HCC.

Although Sorafenib improves overall survival, many patients develop resistance. After the approval of Sorafenib, for about 10 years, none of the clinical trials were successful in identifying a treatment after sorafenib failure. Regorafenib, an analog of sorafenib with improved target affinity and higher potency, was the first

second-line treatment approved for patients who failed sorafenib therapy (Llovet et al., 2021). Later, in addition to regorafenib, cabozantinib (The CELESTIAL trial, ramucirumab (REACH-2 trial) and nivolumab (CheckMate 040 trial) were also approved as second-line treatment options (Abou-Alfa et al., 2018), (Llovet, Villanueva, et al., 2021), (Llovet, Kelley, et al., 2021).

There are also many ongoing Phase 3 trials for second line HCC treatment. Since majority of Phase 3 trials are done after sorafenib failure, sorafenib still remains the globally accepted first-line treatment for advanced HCC despite its poor therapeutic response and high rates of resistance ((Zhu et al., 2018). Thus, identifying mechanisms mediating sorafenib resistance is of crucial importance.

2.1 HCC Tumor Microenvironment

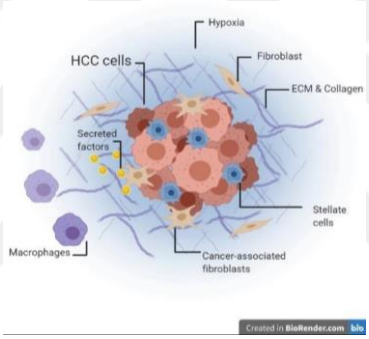

Figure 1. Diagram of tumor microenvironment (TME) of HCC (Nishida et al., 2015).

2.1.1. Cancer Associated Fibroblasts (CAFs)

Cancer Associated Fibroblasts (CAFs) are a specialized group of fibroblasts which have an effect on tumor metastasis and invasion. Several studies indicated that there is a strong correlation between CAFs and poor prognosis in cancer (Liu et al., 2016), (Franco et al., 2010). CAFs express specific mesenchymal markers such as α-SMA, Vimentin, and peri-tumor fibroblast (FSP-1) (Franco et al., 2010). Most HCC develops on fibrotic and/or cirrhotic livers. Myofibroblasts and hepatic stellate cells are the main generators of extracellular matrix in the liver. They are derived from quiescent fibroblast and activated hepatic stellate cells by chronic injury. HCCs were shown to be found in fibroblast rich microenvironment (Mazzocca et al., 2011) α-SMA is the myofibroblast marker that is highly expressed in CAFs compared to normal fibroblasts. In human breast cells, CAFs express TGF-β and hepatocyte growth factor

(HGF) enhancing malignant transformation (Kuperwasser et al., 2004). Also, CAFs stimulate the proliferation and invasivion in HCC (Lin, Chuang and Chuang, 2012). Chemokines secreted by CAFs modulate the inflammatory cells and tumor cells. In ovarian cancer, CCL5 induces tumor growth and invasion (Tsuyada et al., 2012). Liu et al. demonstrated that CAF-derived molecules stimulate HCC metastasis via Hedgehog and TGF-β activation. Also, when HCC cells and CAFs are co-cultured, HCC cell's proliferation, migration, and invasion was augmented (Tsuyada et al., 2012).

2.1.2. Hepatic Stellate Cells (HSCs)

Quiescent stellate cells constitute 5-8% of the liver cells and function in storage and controlled release of retinoids. HSCs secrete significant amounts of extracellular matrix (ECM). They also promote control of blood flow through the sinusoidal capillaries. They are a major source of various paracrine, autocrine and chemoattractant factors for liver homeostasis (Geerts, 2001), (R. Seo, 2015). Also, they were found in many other organs such as kidney, pancreas, and lung (Liu, 2006), (Keane, Strieter and Belperio, 2005). When the liver is scarred by viral infection or hepatic toxins, HSCs transform from quiescent cells to activated myofibroblast-like cells. After that, they significantly upregulate secretion of cytokines, growth factors, and proteins for protecting the liver. This activation, can be detected by morphological changes, an increase in the expression of α-SMA and production of ECM molecules (Friedman, 2008), (Sokolović et al., 2010). The factors released by activated HSCs such as HGF and TGF-β1 can modulate liver regeneration (Chen et al., 2012). By producing growth factors and cytokines such as HGF and IL-6 that can induce phenotypic changes in cancer cells, HSCs also play an important role in liver carcinogenesis. It has been shown that co-culturing of HSCs with Huh7 cells enhances HSC proliferation, migration and expression of pro-angiogenic genes (Sancho-Bru et al., 2010).

2.1.3. Vascular Cells

The transport of nutrients into the liver and the maintenance of the blood flow are managed by the vascular endothelium which is made up of endothelial cells, smooth muscle cells and a basement membrane. Endothelial cells express various receptors for angiogenic factors such as VEGFRs, Tie-2, EGFR, PDGFR. Activation

of these receptors could initiate many signal pathways to control proliferation, invasion and survival. Blood vessels and their cells in tumors were reported to have morphologically abnormal properties (Sancho-Bru et al., 2010), (R. Seo, 2015). The tumor endothelial cells (TECs) can re-enter the circulation and travel to other sites. TECs were also reported to express high amounts of VEGF. VEGF is a major inducer of angiogenesis and is known to contribute to tumor progression by inducing angiogenesis in tumors (Dudley, 2012), (Moens et al., 2014), (Jain, 2009). VEGF induces neovascularization and the VEGF/VEGFR network enhances the tumor growth in HCC. For this reason, targeting the VEGF/VEGFR pathway is one of the main strategies used for HCC treatment in clinical trials. Sorafenib, the multi-kinase inhibitor used in first line treatment of advanced HCC patients, is also an anti-VEGF agent (Finn and Zhu, 2009).

2.1.4. Cancer Stem Cells

Cancer stem cells (CSCs) have self-renewal and differentiation properties like normal stem cells. CSCs were initially discovered in leukemia, but later was discovered in various solid malignancies including various cancer types (Hermann et al., 2007), (Li et al., 2007), (O'Brien et al., 2007). CSCs have extremely increased tumorigenic, metastatic, and chemotherapy and radiation-resistant features. CSCs escape from multiple drug actions with intrinsic and external mechanisms (O'Brien et al., 2007). External mechanisms activate hypoxia, anormal angiogenesis and signalling cascades including epithelial-mesenchymal transition (EMT) (Maugeri-Saccà, Vigneri and De Maria, 2011). Intrinsic mechanisms activate DNA damage repair cascade, expression of MDR proteins and induce the ability of reconstituting tumors, EMT and expression of self-renewal related genes (Calcagno et al., 2010), (Calcagno et al., 2007).

2.1.5. Interaction between HCC and CSCs

Liver cancer stem cells (LCSCs) are the cancer stem cells of HCC. Various surface markers are used to isolate LCSCs. LSCSs have been shown to mediate chemoresistance, metastasis, and recurrence in HCC due to their increased self-renewal and survival capacity. Thus, identifying and targeting LCSCs became an important issue in HCC treatment (Ji and Wang, 2012), (Guo, Lasky and Wu, 2006). (Piao et al., 2012), (Xin et al., 2013), (HA et al., 2011).

2.2. Surface markers of LCSCs

2.2.1. EpCAM

Epithelial cell adhesion molecule (EpCAM), is a glycosylated type I transmembrane protein, initially discovered in epithelial tumors (Philip et al., 2009). Although EpCAM expression is not detectable in normal hepatocytes, a small subset of cells in the adult liver identified as liver stem cells are demonstrated to express EpCAM (Cioffi et al., 2012). EpCAM is believed to involve in many processes including cell-cell adhesion, proliferation, cell cycle, signalling, regeneration, organogenesis, tumorigenesis, migration and differentiation (Fan et al., 2011), (Philip et al., 2009).

2.2.2. CD133

CD133 is a membrane glycoprotein (Peng et al., 2019) that shows expression in nucleus and cytoplasm of several tumors including liver, prostate, colon and pancreatic cancers (Chen et al., 2017), (Glumac and LeBeau, 2018), (Güler, Guven and Oktem, 2019). The CD133+ subpopulation and EpCAM+/CD133+ subpopulation demonstrated stemness properties and have higher tumorigenic capacity (Peng et al., 2019). (Karagonlar et al., 2020). Moreover, high levels of CD133 expression were associated with poor prognosis, low survival and high recurrence suggesting that CD133 may be an appropriate prognostic marker for liver cancer (Peng et al., 2019).

2.2.3. CD44

CD44 is a transmembrane glycoprotein and a receptor for hyaluronic acid (HA). Overexpression of CD44 induces proliferation, migration, and drug resistance of tumor cells (Ma et al., 2007), (Bourguignon, Shiina and Li, 2014). IL-6 secreted by tumor-associated macrophages was shown to increase the percentage of CD44+ population in tumors and enhance tumorigenesis (Wan et al., 2014). Moreover, knockout of CD44 in HCC was associated with an increase in drug sensitivity (Asai et al., 2019)

2.2.4. CD90

CD90 is a membrane protein, which has roles in inflammation, cytoskeleton organization and cell migration. CD90 is expressed in several cell types, including neurons, endothelial cells, astrocytes and fibroblasts (Zhen et al., 2008). CD90 is also

defined as a marker of LCSCs with high tumorigenic and metastatic properties (Chiba et al., 2013).

2.2.5. CD24

CD24 is glycoprotein promoted in B- lymphocytes and is overexpressed in a variety of cancers (Pruszak, Menon and Pruszak, 2017). In HCC cells, CD24 takes part in metastasis, differentiation, self-renewal, and chemoresistance. Besides, expression of CD24 was found to be correlated with PCNA and β-catenin expressions and associated with high metastatic potential (Qiu et al., 2011).

2.3 Immune Cells

In the TME, immune cells consist of macrophages, neutrophils, and lymphocytes. Tumor cells associate with immune cells in the tumor microenvironment and mediate immune escape and tumor suppression (de Mingo Pulido and Ruffell, 2016). Immune cells have the ability to both kill and induce tumor cells, according to the cellular environment (Bhatia and Kumar, 2020), (Galon et al., 2013). Although the immune system destroys highly immunogenic tumor cells, the cancer cells with low immunogenicity tend to escape from immune destruction and stimulate the immune tolerance (Bhatia and Kumar, 2020.Tumor cells can modify the immune system by generating inhibitory cytokines such as interleukin-10 (IL-10), transforming growth factor-β (TGFβ), and vascular endothelial growth factor (VEGF). They also activate immunosuppressive cells such as regulatory T cells (Tregs) and myeloid-derived suppressor cells (MDSCs) and promote an immunosuppressive TME.

2.4. Macrophages

Macrophages control tumor growth, angiogenesis, invasion and metastasis with their dual anti and pro-tumor functions (Maria R. Galdiero et al., 2013), (Condeelis and Pollard, 2006). Tumor-associated macrophages are classified as two types M1 and M2, depending on the phenotypes. Interferon (IFN) γ and lipopolysaccharide (LPS) stimulate M1 cells. M1 cells secrete pro-inflammatory cytokines such as TNFα and IL-12 and process high levels of nitric oxide synthase (NOS) and MHC molecules. They have a significant part in pathogen clearance and tumor antigen presentation. IL-4 and IL-10 activate M2 cells. M2 cells control levels of MHC molecules and IL-12. However, immunosuppression, tumor cell

extravasations, and metastasis are seen upon stimulation with various anti-inflammatory cytokines such as IL-10, mannose receptor and arginases (Condeelis and Pollard, 2006). M2 type is the common type of tumor-promoting tumor-associated macrophages, when M1 and M2 cells are found together in the TME. TME is a dynamic system. In the early phase of tumor initiation, TAMs demonstrate an inflammatory phenotype, on the other hand during tumor progression and metastasis, they show immunosuppressive characteristics (Franklin et al., 2014).

2.5. The Most Reported Signalling Pathways in HCC

Pathways which are important for normal liver development, function and homeostasis, also are frequently deregulated in HCC. Abnormal activation and deregulation of major signalling pathways support tumor initiation, growth and metastasis and contribute to tumor recurrence and therapeutic resistance (Liu, Yeh and Lin, 2020).

2.5.1. Ras/Raf/MEK/ERK Signaling Pathway

The Ras, Raf, MEK and ERK proteins cooperate to control the vital properties of the cell (Li et al., 2016). Ligand binds to tyrosine kinase (RTK), on residue of RTK cytoplasmic tails autophosphorylation occurs therefore activates the Ras, Raf, MEK and ERK respectively. ERK triggers expression of proliferation genes by going into the nucleus. Because of mutations, the main activation of the path is critical to stimulate HSC to fibrogenesis and myofibroblast phenotype (Lee, Mstp and Friedman, 2011).

2.5.2. PI3K/AKT Signaling Pathway

Phosphatidylinositide 3-kinases (PI3K) phosphorylates the phosphatidylinositol (4,5)-bisphosphate (PIP2) to phosphatidylinositol (3,4,5)-trisphosphate (PIP3). After RTK-ligand interaction, PI3K is another target of RTKs. PTEN is a tumor suppressor which reverses the pathway. PIP3 level is low in unstimulated conditions of normal cells (Hemmings and Restuccia, 2012). In HCC patients, deregulated PIP3-AKT-mTOR was observed (Tovar et al., 2009).

2.5.3. TGF-β Signaling Pathway

Transforming growth factor-β (TGF-β) is critical for cell. There are more than

30 proteins in the TGF-β family, which also contains myostatin, activin, inhibin, nodal and bone morphogenetic proteins. TGF-β binds to kinases on the membrane and stimulates signalling. Thus, an activated ligand is able to connect TGF-β receptors and send the signal to the nucleus using Smad proteins (Weiss and Attisano, 2013). TGF-β plays dual role in HCC progression, in early stages it is a tumor suppressor while stimulating metastasis at early stages. In the tumor microenvironment, there is a positive correlation between tumor-associated macrophages (TAMs) which are critical parts of immune cells and EpCAM positive cell populations (Meindl-beinker and Matsuzaki, 2012).

2.5.4. The Wnt/β-Catenin Pathway

Wnt/β-catenin signaling has an important role in homeostasis (Mohammed et al., 2016). β-catenin is a functional protein with a role in cell–cell adhesion and also serves as a transcription factor. In the Wnt signaling pathway it acts as an intracellular signal transducer (Macdonald, Tamai and He, 2009). Also, β-catenin is one of the subunits of cadherin that binds E-cadherin but mutation and overexpression of β-catenin supports tumor progression and growth (Gedaly et al., 2014). In HCC patients, β-catenin accumulation is seen in about 50% of cases (Yamashita et al., 2021).

2.5.5. Signaling Pathway of p53

The p53 is a tumor suppressor gene which has a critical role in cell cycle progression and cell division by modulating the transcription of growth regulatory genes. p53 protein is significantly upregulated by DNA damage, hypoxia, viral proteins, or oncogene expression (Vousden, 2000). Mutations in the p53 gene lead to genomic instability and loss of normal functions such as growth control, cell cycle arrest or apoptosis (Chen et al., 2003). The p53 gene is frequently mutated in humans and it has an important role in early stages of HCC. p53 mutations can be detected in about 50% HCC cases (Whittaker, Marais and Zhu, 2010).

2.5.6. The Notch Signalling

The vital functions of the cell are regulated by the Notch signalling. It influences tumor progression, self-renewal, and CSC differentiation in most cancer types. Notch and Wnt/β-catenin signaling pathways have both critical roles in stemness and metastasis of liver cancer stem cells. Notch1 is upregulated and triggers

NICD expression in HCC via Wnt/β-catenin signaling. Blocking the Wnt/β-catenin and Notch signaling pathways mediates suppression of tumor growth (Farazi and Depinho, 2006).

2.5.7. Hedgehog Signaling Pathway

It controls cell proliferation, survival, and differentiation (Serova et al., 2015). Overexpression of Hh ligands results in abnormal transcription factor expression and is detected in the development of several cancer types such as breast cancer, prostate cancer, HCC, pancreatic cancer, and brain cancers (Mcnamara et al., 2015). In HCC, the Hh markers are overexpressed in tumors with vascular invasion and metastasis and correlated with recurrence with low survival rate (Zhu et al., 2021).

2.6. HCC Studies in 2D and 3D Cell Culture

Over the decades two-dimensional (2D) monolayer cell culture methods were used to understand cell function *in vitro*. However, standard *in vitro* tumor models are not enough to generate cellular and spatial complexity efficiently (Hutchinson and Kirk, 2011). It is clear that enhanced multicellular in vitro models are necessary for understanding the basic tumor-stroma interactions and its effects on tumorigenic phenotypes. In 2-D cell culture, interactions between cells are relatively absent inhibiting them from cytokines, growth factors, and signalling molecules. Although 2D models are simple and cheap, cells are seeded on glass or plastic materials and thus these models do not demonstrate real properties of tissues (Yamada and Cukierman, 2007), (Antoni et al., 2015). In 2D culture, different gene expression patterns, morphology, cellular architecture (cell-cell and cell-ECM interactions) are seen (Breslin & O'Driscoll, 2013). Drug metabolism of cancer cells is changed by lack of signalling, thus 2D culture is not a good system for drug development research (Kapałczyńska et al., 2018). Generally animal models are used for in vivo experiments; however, concerns about animal testing and high cost avoid high use of animals (Cekanova and Rathore, 2014). That's why more accurate models such as three-dimensional (3D) cell culture is needed to mimic tumor microenvironment effectively. 3D models aim to focus directly on human models by removing obstacles from different species and mimic tumor microenvironment. In multicellular organisms, cells tend to make arrangements with each other and environment also, they exchange chemicals and nutrients so maintain homeostatic balance. Thus, regulation of cells is

the main criteria considered to be an ideal organisation in the 3D culture (Lee, Cuddihy and Kotov, 2008), (Abbott, 2003). This helps to understand ECM expression, cell-cell and cell-matrix interactions (Figure 1). 3D cultures canalize cells to become spheroids by secreting extracellular matrix contents. Spheroids have similar properties with in vivo cell microenvironment. Spheroid cultures are good candidates for studying cancer and also for preclinical drug development studies. In 3D systems, cells activate the development of aggregates/spheroids in matrices or media (Figure 2). In spheroid models, interactions between cell-cell and cell-matrix are not completely mimicking but, to some degree, these models are convenient to activate the morphology of cells according to the original state in the body. In addition, there are several phases of cells that are related to oxygen and nutrition levels (Khaitan et al., 2006). Proliferation mostly occurs at the outer surface of the spheroids as they reach an adequate number of nutrients and oxygen from the media. Due to deficiency of nutrients, oxygen and growth signals, in the inner parts of spheroids cells become hypoxic (Senkowski et al., 2016) (Figure 3).

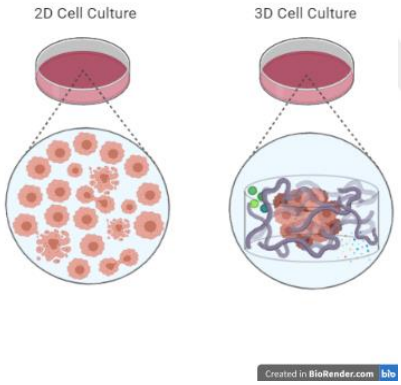

Figure 2. Schematic representation of differences between 2D and 3D cell cultures. In monolayer cell culture, interaction between different cells and stroma is absent. In 3D cell culture, cell-cell and cell-ECM communication provide cells with growth factors and cytokines.

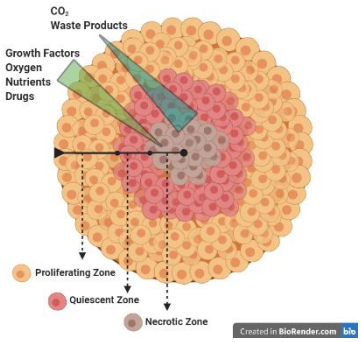

Figure 3.The structure of three-dimensional spheroids. The regions are colored as the proliferating zone (orange), quiescent zone (red), and necrotic zone (brown).

CHAPTER 3: MATERIALS AND METHODS

3.1 Cell Culture

Huh7, sorafenib resistant Huh7 (Huh7-SRC5), THP1 and LX-2 cell lines were used in our study. Huh7, Huh7-SRC5 and THP1 cell lines were cultured with RPMI-1640 containing a mixture of 10% FBS (Fetal Bovine Serum), 2mM L-Glutamine, 100µ / ml penicillin / 0.1mg / ml streptomycin and 1% non-essential amino acid mixture in an incubator with 5% CO_2 at 37 ^oC. The LX-2 cell line was cultured in DMEM containing 2% FBS (Fetal Bovine Serum), 2mM L-Glutamine, 100u / ml penicillin / 0.1mg / ml streptomycin and 1% non-essential amino acid mixture in an incubator with 5% CO_2 at 37 ^oC. Sorafenib was used in the maintenance of the sorafenib resistant cell lines and in the experiments at a final concentration of 5 µM.

3.2 Proliferation Analysis using MTT

MTT is used for measuring cytotoxicity, proliferation and cell viability. In metabolically active cells, yellow tetrazolium salt (3-(4,5-dimethylthiazol-2-yl)-2,5-diphenyltetrazolium bromide or MTT) transform into purple formazan crystals. MTT was performed to analyse the effects of Sorafenib and Regorafenib on cell proliferation. Cells were seeded as $3x10^4$/100 ul in all MTT analyses. Regorafenib and Sorafenib were administered the next day after seeding. On the day of analysis, 15 µl of MTT (5 µg / ml) solution was added to each well. The plate was incubated for 4 hours at 37ºC in a CO2 incubator. Then the medium was removed from each well, 100 µl DMSO was added and incubated for 30 minutes in a shaker protected from light. Measurements were made using a spectrophotometer (Multiscan GO Thermo Scientific, Porto Salvo) at 570 nm wavelength. Spectrophotometric measurements were also taken at 720 nm wavelength for the background. The evaluation of cell viability was calculated using the nonlinear regression method by converting the values obtained through the Graphpad Prism program to logx format.

3.3 Three-Dimensional Hanging Drop Spheroid Cell Culture

3.3.1 Preparation of a Single Cell Suspension

Adherent cells with 90% confluence were rinsed with PBS. 1 ml of 0.25% trypsin-EDTA was added and incubated at 37°C until cells detach. Trypsinization was stopped by addition of 3 ml of complete medium and cells were pipetted gently using

a 5 ml pipette until cells were in suspension. Cells were then transferred to a 15 ml conical tube and centrifuged at 1000 rpm for 4,5 minutes. Supernatant was discarded and cells were suspended with complete tissue culture medium. By using a hemocytometer, cells were counted. and calculated as required by the experiment. (For example, Huh7 cells were calculated as 700 cells/30 µl, LX-2 cells were calculated as 200 cells/30 µl and THP-1 cells were calculated as 100 cells/30 µl.)

3.3.2. Formation of Hanging Drops

6 ml of PBS was placed in the bottom of a 10 cm dish. This acted as a hydration chamber. The lid of the dish was then inverted to deposit 30 µl of cell mixture drops onto the inside of the lid. Lastly, the lid was inverted carefully again onto the PBS-filled plate and placed in an incubator with 5% CO2 at 37ºC.

3.4. Immunofluorescent Analysis of Spheroids

On Day 1, spheroids were taken into a falcon tube. Medium was removed by using a pipette and spheroids were washed with 500 µl PBS three times. Spheroids were then fixed with 4% paraformaldehyde for 1 hr at 4°C. The spheroids were then washed thrre times with 1XPBS. 500 ul of Permeabilization Buffer (8% SDS in 0.1M PBS (pH 7.5)) was added onto the spheroids and left at 4°C overnight. On Day 2, permeabilization buffer was removed and spheroids were rinsed 3 times with PBS for 3 hours, then incubated in blocking buffer (0.5% (v/v) Tween 20 + 0.2% (v/v) Triton X-100 + 3% BSA)) for 2 hours. After blocking, the primary antibody to be used was diluted 1:50 in the blocking buffer and added onto spheroids overnight at 4°C. On Day 3, spheroids were washed with wash buffer (0.1% (v/v) Tween 20 + 0.2% (v/v) Triton X-100 + PBS) for three times, each time for 1 hr at room temperature. Then, a secondary antibody (1:1000 diluted) and DAPI (1:5000 diluted) was mixed together in the blocking buffer. Wash buffer was removed and 100 µl of the secondary antibody/stain mixture was added to each well. Spheroids were incubated overnight at 4°C (without rocking). On Day 4, spheroids were washed with 100 µl of 1xPBS for 1 hr at RT in the dark. 1XPBS was then removed, spheroids were incubated with Refractive Index Matching Solution (50% formamide/20% polyethylene glycol (PEG)) for 1 hour. Spheroids were then transferred in a small amount of buffer to a Superfrost microscope slide. 10 µl of Refractive Index Matching Solution was added to cover the spheroid, and coverslips were gently placed on top. For sealing the

coverslips, nail polish was used and prepared slides were left in the dark for approximately 30 minutes. When slides had dried, image analysis was carried out using a confocal microscope (Zeiss LSM880, Jena Germany).

3.5. Lentiviral Transduction

On Day 0, HEK293T cells were seeded at 3.8×10^6 cells per plate in high glucose DMEM (w/ %10 FBS) in 10 cm tissue culture plates. Up to P15 passage cells were used for transfection. Then, 293T cells were seeded onto gelatin or poly-l-lysine coated plates and incubated at 37 ℃, 5% CO2 for approximately 20 hours. On Day 1, media was gently aspirated and fresh DMEM (w/ %10 FBS) was added 5 hours before the transfection. Then a mixture of 3 transfection plasmids (3,4 µg plasmid, 1,7 µg of psPAX2 and 0,85 µg of PMD2.G) was prepared in 300 µl of 1XPBS. PEI mix (300 µl of 1XPBS and 30 µl of PEI) was also prepared, vortexed and later added drop by drop to plasmid mix. The final mix was vortexed and incubated for 15-20 min in RT. This mix was added onto the 293T cells dropwise in the clock direction while rotating the plate opposite to clock direction. On Day 3, the medium was replaced with fresh medium. On Day 4, the virus was harvested (48 hours after transfection). Supernatant was filtered through a 0.45 µm PES filter and filtered viral supernatant was added onto Huh7, Huh7-SRC5, LX-2 and THP-1 cells with polybrene (8 ug/µl). Next morning media was aspirated, and 10 mL of fresh RPMI (w/ %10) was added onto cells. Huh7-mCherry, Huh7-SRC5-mcherry, LX-2 Azurite and THP-1- GFP cell lines were produced.

3.6. Immunofluorescent Analysis of Activated LX-2 Cells

On the Day 1, for the seeding process; in the class II biological safety cabinet, LX-2 cells were seeded on coverslips in a 24-well plate at a density of $4x10^4$ cells/well using DMEM with 0.5% FBS and incubate cells overnight. On the Day2, medium was replaced with serum-free DMEM containing TGF-β1 (10 ng/ml) and the cells were incubated for 24 hours. On the Day 3, medium was removed and cells were washed 3 times with each time 500 µl PBS then removed PBS. Both control and PMA-treated cells were fixed with 4% paraformaldehyde for 15 minutes at 4°C. Paraformaldehyde was removed by using a pipette and discarded in a chemical waste bin. Cells were washed three times with 1X PBS. After this step, a permeabilization buffer (PBS containing 0.5% (v/v) Tween 20 + 0.2% (v/v) Triton X-100) was added to cells at RT

for 15-20 min. Then, the permeabilization buffer was removed and 200 µl of blocking buffer (PBS containing 0.5% (v/v) Tween 20 + 0.2% (v/v) Triton X-100 + 3% BSA) was applied for 1-2 hrs at RT. Coverslips were transferred to a humidity chamber (150 mm petri dish with moist blotting paper + layer of parafilm + labelled spaces for coverslips). Coverslips were laid cell-side-up on the parafilm. Primary antibody was diluted 1:50 in blocking buffer and added 100 µl of the primary antibody dilution and incubated cells overnight at 4°C. (Primary antibody: α-SMA) On the Day 4, cells were washed with immunofluorescence wash buffer (0.1% (v/v) Tween 20 + 0.2% (v/v) Triton X-100 + PBS) three times, each time for 15 min at room temperature. Secondary antibodies (1:1000) and DAPI (1:5000) were mixed together in the blocking buffer. Wash buffer was removed and 100 µl/well of the secondary antibody/stain mixture prepared. The plate was covered with foil and the cells were incubated at room temperature for 2 hours (without rocking). Cells were washed with 100 µl of 1xPBS for 1 hr at room temperature in the dark. 1XPBS was removed, cells were incubated with Refractive Index Matching Solution (50% formamide/20% polyethylene glycol (PEG)) for 1 hour. Cells were transferred in a small amount of buffer to a Superfrost microscope slide and 10 µl of Refractive Index Matching Solution was added to cover cells. hen a coverslip was placed on top and for sealing coverslip on the slide nail polish was used and left in the dark for approximately 30 minutes. When slides dried, image analysis was carried out (Zeiss LSM880, Jena Germany).

3.7. Immunofluorescent Analysis of Activated THP-1 Cells

On Day 1, THP-1 cells were seeded on coverslips in a 24-well plate at a density of 10^5 cells/well (100 000 cells/500µl). 150 µM phorbol 12-myristate 13-acetate (PMA, Sigma, P8139) was prepared. For each well 1 µl from 150 µM PMA with 499 µl RPMI Medium were mixed. (Each well already had 500µl Media+ cells, thus the final dilution was 1:1000 and final PMA concentration was 150nM). Cells were incubated with PMA for 2 days. Then, fresh medium was added and incubated for another 24 hours. On the Day 4, for control cells, 5ml fresh THP-1 cell suspension was taken and counted. Then, 100 000 cells/ 30 µl was prepared and added as a drop of cells onto a coverslip, dried for 15 min. For PMA treated cells, medium was removed and cells were washed 3 times with each time 500 µl PBS. Both control and PMA-treated cells were fixed with 4% paraformaldehyde for 15 minutes at 4°C. Paraformaldehyde was removed by using a pipette and discarded in a chemical waste

bin. Cells were washed three times with 1XPBS. After this step, a permeabilization buffer (PBS containing 0.5% (v/v) Tween 20 + 0.2% (v/v) Triton X-100) was added to cells at RT for 15-20 min. Then, the permeabilization buffer was removed and 200 µl of blocking buffer (PBS containing 0.5% (v/v) Tween 20 + 0.2% (v/v) Triton X-100 + 3% BSA) was applied for 1-2 hrs at RT. Coverslips were transferred to a humidity chamber (150 mm petri dish with moist blotting paper + layer of parafilm + labelled spaces for coverslips). Coverslips were laid cell-side-up on the parafilm. Primary antibody was diluted 1:50 in the blocking buffer and 100 µl of the primary antibody dilution was added overnight at 4°C. (Primary antibody: anti-CD68) On Day 4, cells were washed with immunofluorescence wash buffer (0.1% (v/v) Tween 20 + 0.2% (v/v) Triton X-100 + PBS) three times, each time for 15 min at room temperature. Secondary antibodies (1:1000) and DAPI (1:5000) were mixed together in the blocking buffer. Wash buffer was removed and 100 µl/well of the secondary antibody/stain mixture was prepared. The plate was covered with foil and the cells were incubated at room temperature for 2 hours (without rocking). Cells were washed with 100 µl of 1xPBS for 1 hr at room temperature in the dark. 1XPBS was removed, cells were incubated with Refractive Index Matching Solution (50% formamide/20% polyethylene glycol (PEG)) for 1 hour. Cells were transferred in a small amount of buffer to a Superfrost microscope slide and 10 µl of Refractive Index Matching Solution was added to cover cells. Then a coverslip was placed on top and for sealing coverslip on the slide nail polish was used and left in the dark for approximately 30 minutes. When slides dried, image analysis was carried out (Zeiss LSM880, Jena Germany).

3.8. Flow Cytometry

Spheroids were collected and washed with 1X PBS. Then spheroids were dissociated with 1 ml of 1X Trypsin for 5-10 minutes using thermoshaker at 37ºC. 3 ml of DMEM with 10% FBS was added and single cell suspensions were passed through a 100 micron cell strainer. Cells were counted using Trypan Blue and prepared as 10^5-10^6 cells/300 ml. Cells were then stained with the conjugated primary antibodies for 30 minutes on ice at dark. After being washed 3 times with PBS, cells were analysed via Flow Cytometry (BD LSR FORTESSA, United States).

3.9. Cytokine and Kinase Array

3.9.1. Cytokine Array

Proteome Profiler Array Human XL Cytokine Array Kit (Minneapolis US) was used for Cytokine arrays. Before starting, all array buffers (ABs) were brought to room temperature. Spheroids cultured as droplets in DMEM (10%FBS) for 7 days. Then spheroids were transferred into poly-hema coated plates and cultured in low serum DMEM (2%FBS) for 16 hours. Next day, 1 ml of conditioned medium was collected from spheroids and was mixed with 500µl of AB6. Each membrane was blocked in 2 ml of AB6 for 1 hour on a shaker. After blocking, AB6 was aspirated from the wells and 1.5 ml of conditioned media (1 ml of conditioned medium+500µl of AB6) was added and membranes were incubated overnight at 4 °C on a shaker. Next day, each membrane was washed three times with 20 ml of 1X Wash Buffer for 10 minutes each on a shaker. Membranes were then incubated with a detection antibody cocktail for 1 hour on a shaker. Membranes were then washed three times as described above. Then each membrane was incubated with 2.0 ml of 1X Streptavidin-HRP for 30 minutes at RT on a shaker. Membranes were then washed three times as described above. Each membrane was then placed on the bottom sheet of the plastic sheet protector and 1.0 ml of the Detection Reagent Mix (1:1) was evenly pipetted onto each membrane. After incubation for 1 minute, membranes were visualized using the Vilber Fusion Solo S system (Vilber Lourmat).

3.9.2. Kinase Array

Proteome Profiler Array Human Phospho-Kinase Array Kit (Minneapolis US) was used for the Kinase array. Before starting, all array buffers (ABs) were brought to room temperature. Spheroids cultured as droplets in DMEM (10%FBS) for 7 days were washed with 1X PBS and immediately lysed in the lysis buffer provided with the kit (with phosphatase and protease inhibitors added). 334 µl of lysate was mixed with 1.700 µl of AB 1. Each membrane was blocked in 1 ml of AB1 for 1 hour on a shaker. After blocking, AB1 aspirated from the wells and 2 ml of cell lysate in AB6 (334 µl of lysate was mixed with 1.700 µl of AB 1) was added and membranes were incubated overnight at 4 °C on a shaker. Next day, each membrane was washed three times with 20 ml of 1X Wash Buffer for 10 minutes each on a shaker. Membranes were then incubated with detection antibody cocktails (Cocktail A and Cocktail B) for 2 hours at RT on a shaker. After the incubation, the corresponding parts (A and B) of the

membrane were washed separately as described above. Then the membranes were incubated with 1.0 ml of 1X Streptavidin-HRP for 30 minutes at RT on a shaker. Membranes were then washed three times as described above. Corresponding Part A and Part B membranes were placed end-to-end on the bottom sheet of the plastic sheet protector and 1.0 ml of the Detection Reagent Mix (1:1) was evenly pipetted onto each membrane. After incubation for 1 minute, membranes were visualized using the Vilber Fusion Solo S system (Vilber Lourmat).

CHAPTER 4: RESULTS AND DISCUSSION

4.1 MTT Analysis of Huh7 and Sorafenib Resistant SRC Cells

Sorafenib resistant cell line SRC was previously established in our laboratory (Firtina Karagonlar et al., 2016). MTT analysis of the Huh7 parental cell line and its SRC resistant clone was performed using both Sorafenib and Regorafenib (Figure 1). With these results, the IC50 value of the Huh7 parental cell line for Sorafenib was determined as 2.38, while the IC50 value of the SRC clone was determined as 6.945. This analysis confirmed that the SRC clone was a highly sorafenib resistant clone. In addition, the IC50 values of the same cells for Regorafenib were determined as 1.732 for the parental and 2.796 for the sorafenib resistant clone SRC, respectively (Figure 4). This indicated that sorafenib resistant cells also acquired Regorafenib resistance. This finding has not been reported in the literature and supports the main argument of this thesis.

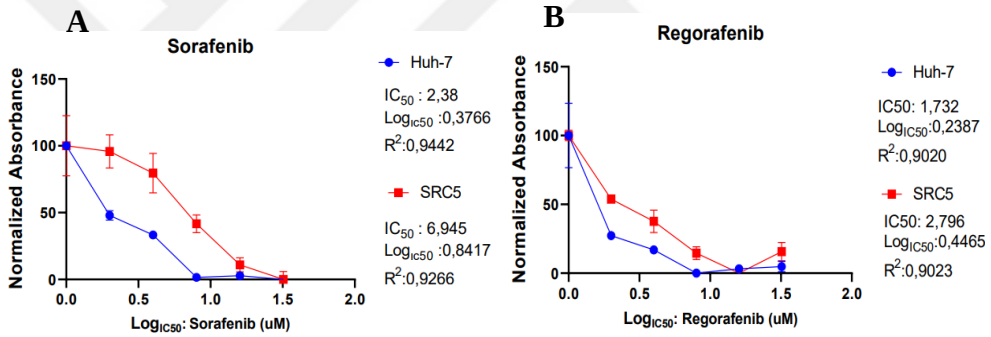

Figure 4. MTT analysis of parental Huh7 cells and Sorafenib resistant clones after Sorafenib (A) and Regorafenib (B) treatment.

4.2. Generation of 3D Tumor Spheroids with Huh7 and Sorafenib resistant SRC Cells

4.2.1 Growth and characterization of cells

We wanted to co-culture Huh7 hepatocellular carcinoma cells with LX-2 hepatic stellate cells and THP1 monocyte cells in order to mimic tumor heterogeneity. Firstly, 3 cell lines were cultured and visualized individually in cell culture using the following media: RPMI with 10% FBS for Huh7, DMEM with 2% FBS for LX-2 and RPMI with 10% FBS for THP-1 cells (Figure 5).

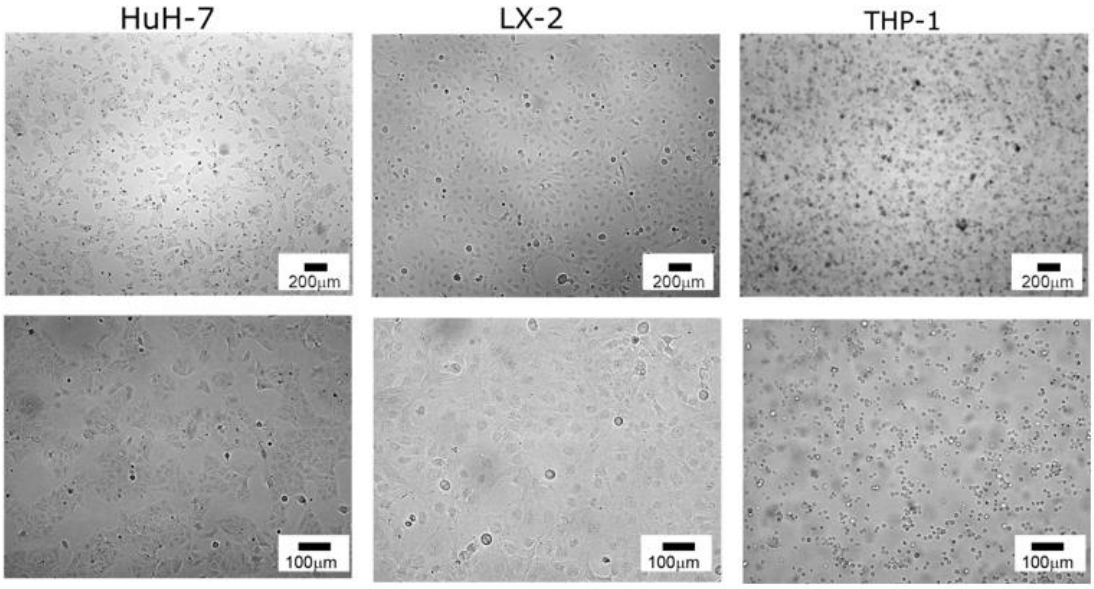

Figure 5. Bright field images of Huh-7, LX-2 and THP-1 cells.

4.2.2 Generation of spheroids

First, spheroid forming capacities of these cells were examined separately. To form spheroids, the hanging drop method was performed using 10 cm cell plates. Huh7, LX-2 and THP1 cells were prepared as 1000 cells in a total of 30 µl medium and were pipetted as 30 µl droplets to the inside of the lid of a 10 cm cell plate. Then, the lid was turned upside down and slowly closed into a 10 cm dish containing 6 ml of 1% PBS (Figure 6). The cell plate was placed in the incubator and incubated at 37°C, 5%CO_2, the spheroids were visualized on days 1,2,3, 4 and 7 (Figure 7). These experiments revealed that epithelial Huh7 cells form significantly bigger spheroids than fibrotic LX-2 cells. On the other hand, THP-1 monocytes which normally grow in suspension do not form compact spheroids.

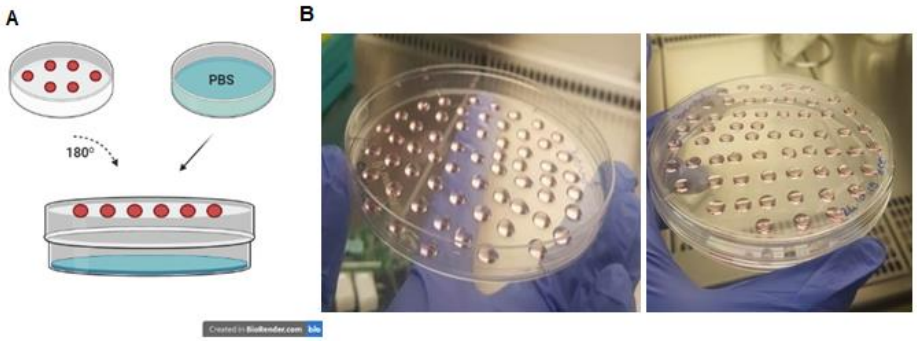

Figure 6. Hanging Drop Method used to generate spheroids. (A) Schematic overview of hanging-drop technique (B) The picture of a 10 cm plate after the pipetting of the droplets.

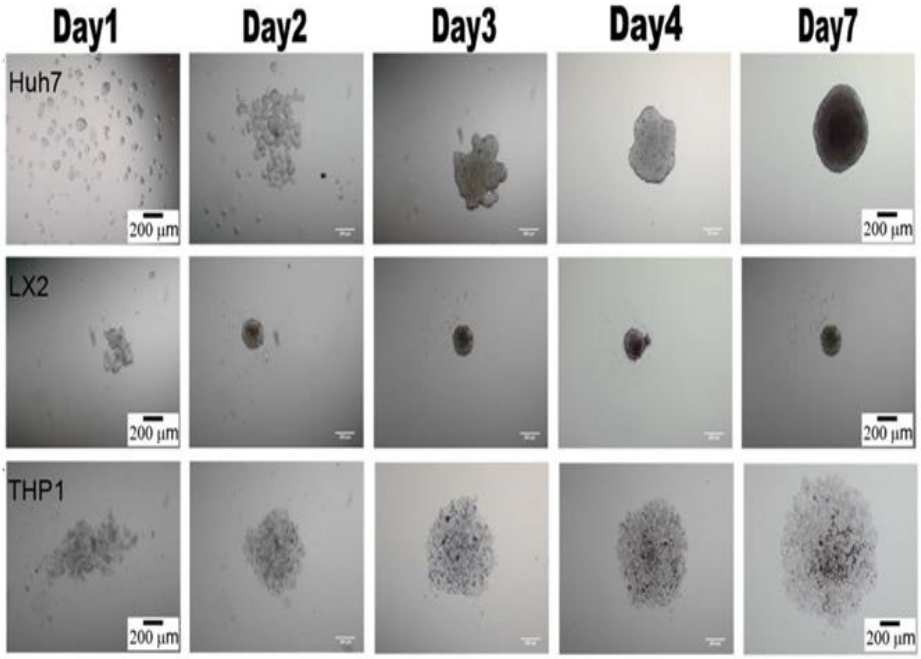

Figure 7. Spheroids formed by the Huh7 cells alone, LX-2 cells alone and THP1 cell lines alone.

In order to mimic tumor heterogeneity, we decided to co-culture all 3 cell types (Huh7, LX-2 and THP-1) in a spheroid. Optimization experiments were carried out to determine how much of each cell type to use. In these experiments the percentages of cell populations in the liver native cell composition were considered. Liver non-parenchymal cells (HSCs, macrophages, endothelial cells, etc.) make up about 30 % of the liver whereas hepatocytes make up 70% of the liver. Thus, in our experiments, we used non-liver parenchymal cells (stellate + macrophage) around 30 % of the total cell number. Accordingly, the following cell numbers were tried and the formed spheroids were visualized (Figure 8-9).

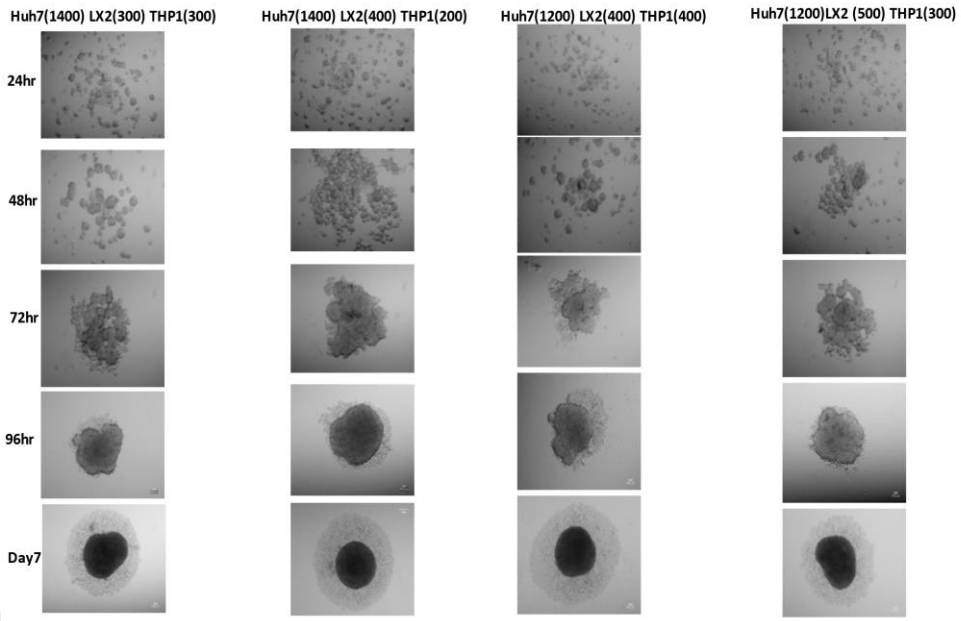

Figure 8. Spheroids created by mixing Huh7, LX-2 and THP1 cell lines with different cell numbers.

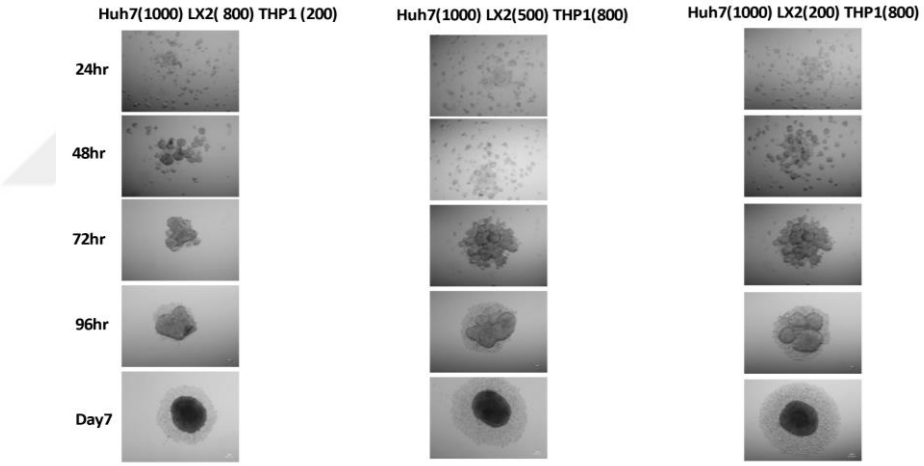

Figure 9. Spheroids created by mixing Huh7, LX-2 and THP1 cell lines with different cell numbers.

In these experiments, when the total number of cells used was 2000, the spheroid diameter was measured above 500 µm. Due to deficiency of nutrients, oxygen and growth signals, in the inner parts of spheroids cells become hypoxic. Therefore, we decided to reduce the total number of cells to 1000 in the future experiments. In a total of 1000 cells, we included 700 Huh7 cells, 200 hundred LX-2 cells and 100 hundred THP-1 cells to form spheroids (Figure 10).

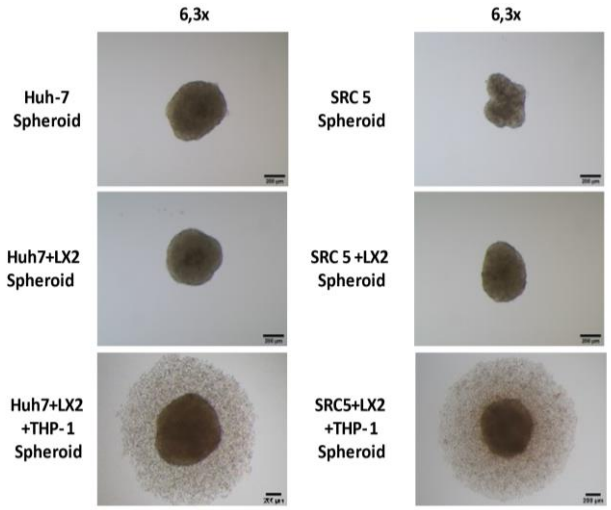

Figure 10. Spheroids formed by mixing with LX-2 and THP1 cell lines, as Huh7 cell number 1000 (Huh7 spheroid, SRC5 spheroid, Huh7+LX-2 spheroid, SRC5+LX-2 spheroid, Huh7+LX-2+THP1 spheroid, SRC5+LX-2+THP-1 spheroid).

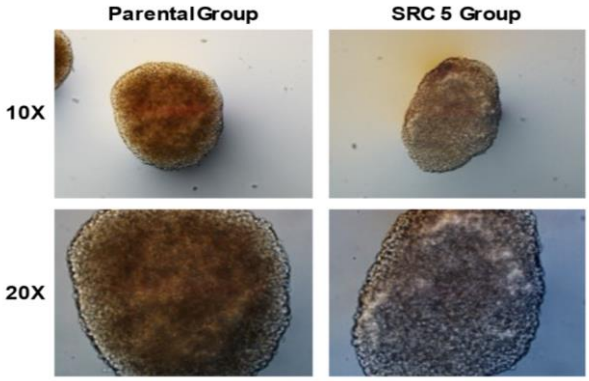

Figure 11. High resolution images of parental (Huh7+LX-2+THP-1 cells) and SRC5 (SRC5+LX-2+THP-1 cells) spheroids.

4.2.3 Regorafenib treatment of spheroids

In order to analyse the effect of regorafenib on parental and resistant spheroids, we performed optimization experiments for regorafenib treatment. Firstly, spheroids were collected from hanging droplets on the 7th day and dispensed into the wells of 96 well plates. The control group was cultured in DMEM-10% FBS without Regorafenib while the drug group was incubated with 2 microMolar Regorafenib in DMEM-10% FBS for 14 days. Spheroids were visualized under the light microscope at day 14, which was after 7 days of Regorafenib treatment and at day 21, which was after 14 days of Regorafenib treatment (Figure 12).

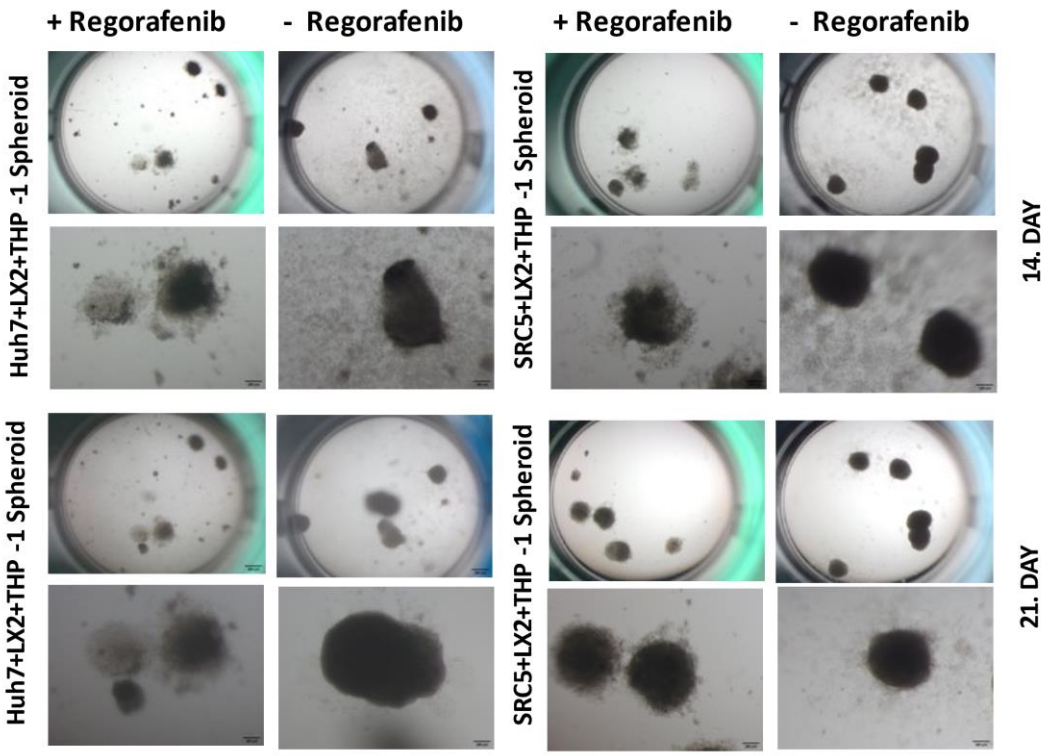

Figure 12. Parental (Huh7+LX-2+THP-1 cells) and SRC5 (SRC5+LX-2+THP-1 cells) spheroids were treated with Regorafenib for 7 days after being transferred to standard cell culture multiwell plates and were visualized under the light microscope on the 14th and 21st day of culture.

We observed that the spheroids that were transferred to standard cell culture multiwell plates showed a tendency to spread and stick to the wells again. For this reason, we decided to try different methods (ULA plate, poly-hema coated plate, treatment while still suspended in droplet). In addition, since it was observed that the spheroids that were not treated with Regorafenib began to look unhealthy during the incubation period of 21 days in total, we decided to end the experiments and perform the analyses on the 14th day (after 7 days of Regorafenib treatment).

We then tried to transfer spheroids into ULA plates on day 7 (Figure 13). Spheroids in the ULA plates still showed a tendency to stick to each other and to the plate edges. In addition, since it was observed that spheroids formed with SRC cells were not affected, we decided to increase the Regorafenib concentration from 2 micromolar to 4 micromolar.

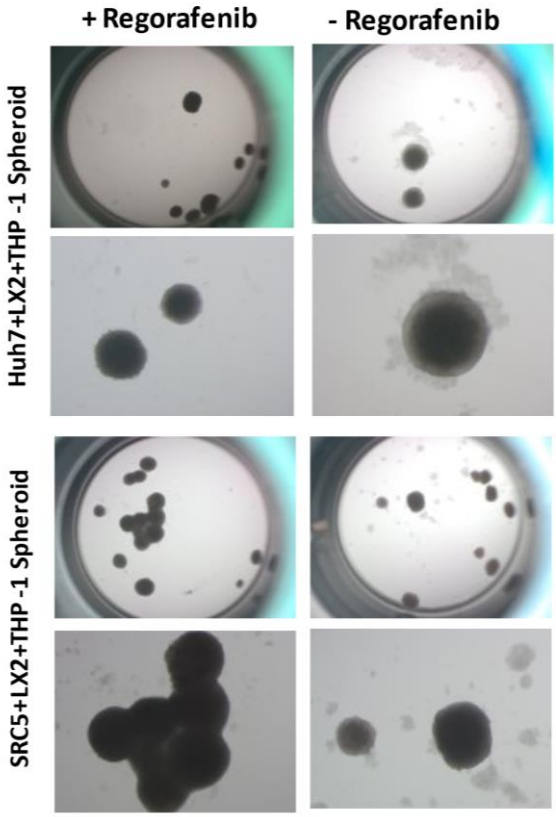

Figure 13. Parental (Huh7+LX-2+THP-1 cells) and SRC5 (SRC5+LX-2+THP-1 cells) spheroids were treated with Regorafenib for 7 days in the ULA plates and were visualized under the light microscope on the 14th day of culture.

As another method, treatment with Regorafenib while the spheroids are in suspended droplet form has been tried. After the spheroids were formed, on the 7th day, the droplet was withdrawn as slowly as possible without disturbing the spheroids, DMEM containing 4 micromolar Regorafenib was added, and the spheroids were incubated with Regorafenib medium as a suspended droplet. Spheroids in the suspended droplet were visualized under the light microscope at day 14 after 7 days (Figure 14). Unfortunately, the effect of Regorafenib was significantly reduced under these conditions.

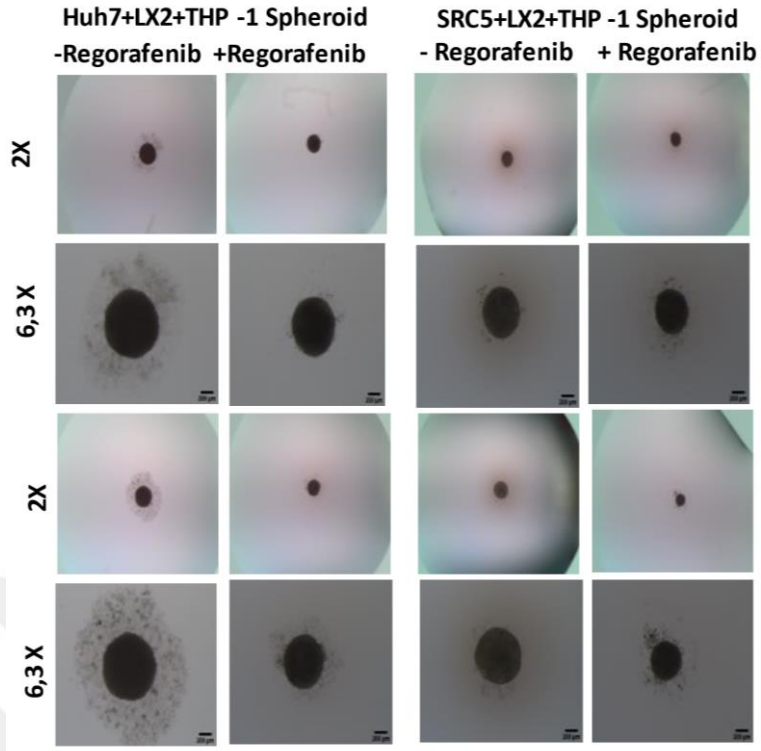

Figure 14. Parental (Huh7+LX-2+THP-1 cells) and SRC5 (SRC5+LX-2+THP-1 cells) spheroids were treated with Regorafenib for 7 days while they are still in suspended droplet form and were visualized under the light microscope on the 14th day of culture.

Moreover, we observed that THP1 (monocyte) cells proliferate much faster than other cell types (Huh7 and LX2) in the spheroids. Also, THP1 cells did not get into the spheroids well, but rather stayed on the outside of the spheroids. It has been observed that the presence of proliferating THP-1 cells on the outer surface of spheroids affected the results of the analyzes with spheroids (Figure 15). Especially by growing on the spheroid, these cells made both the structural analysis of spheroids and the effect of drug treatment difficult. In addition, the presence of THP1 cells created a problem in the preparation of single cell suspension of spheroids for various analyses such as flow cytometry. For this reason, for some experiments, it was decided to establish spheroids without THP-1 cells and to perform analyses on spheroids without THP-1 cells. Firstly, after the spheroids without THP-1 cells were formed, we treated them with 4 micromolar Regorafenib in poly-hema coated plates for 7 days. They were then visualized under the light microscope on day 14 (Figure 16). When the THP-1 cells were not included, the spheroids did not have the growth of cells we observed outside of the spheroids and Regorafenib treatment was more successful.

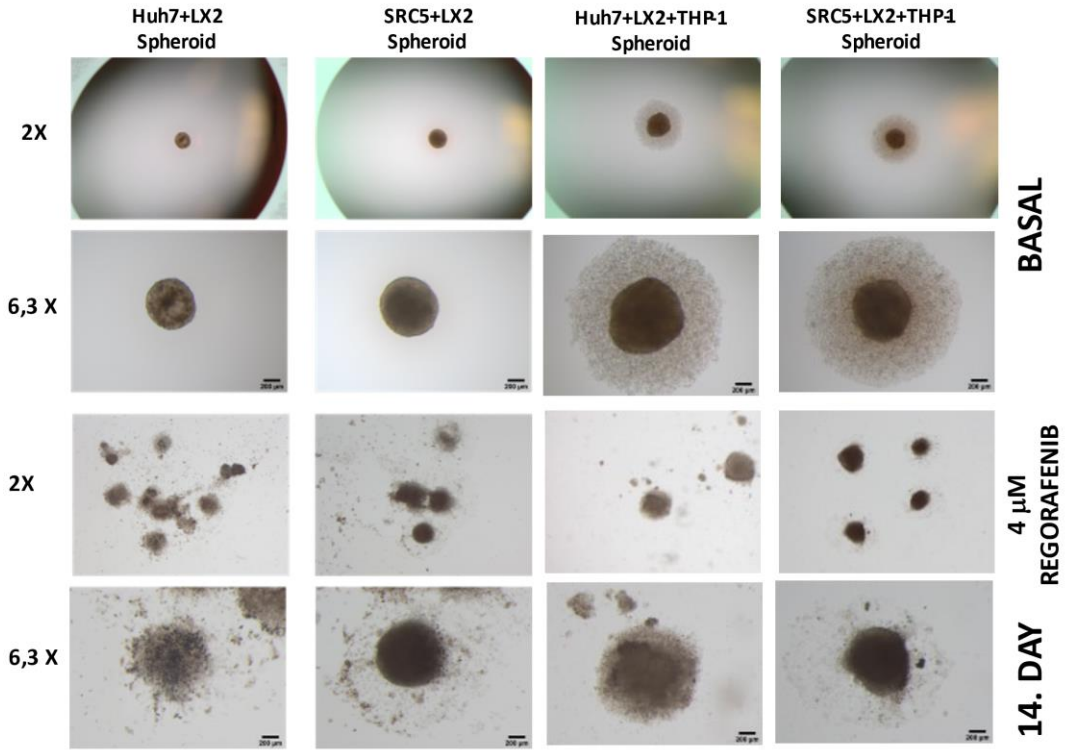

Figure 15. Parental (Huh7+LX-2+THP-1 cells) and SRC5 (SRC5+LX-2+THP-1 cells) spheroids were treated with Regorafenib for 7 days in the poly-HEMA coated plates and were visualized under the light microscope on the 14th day of culture.

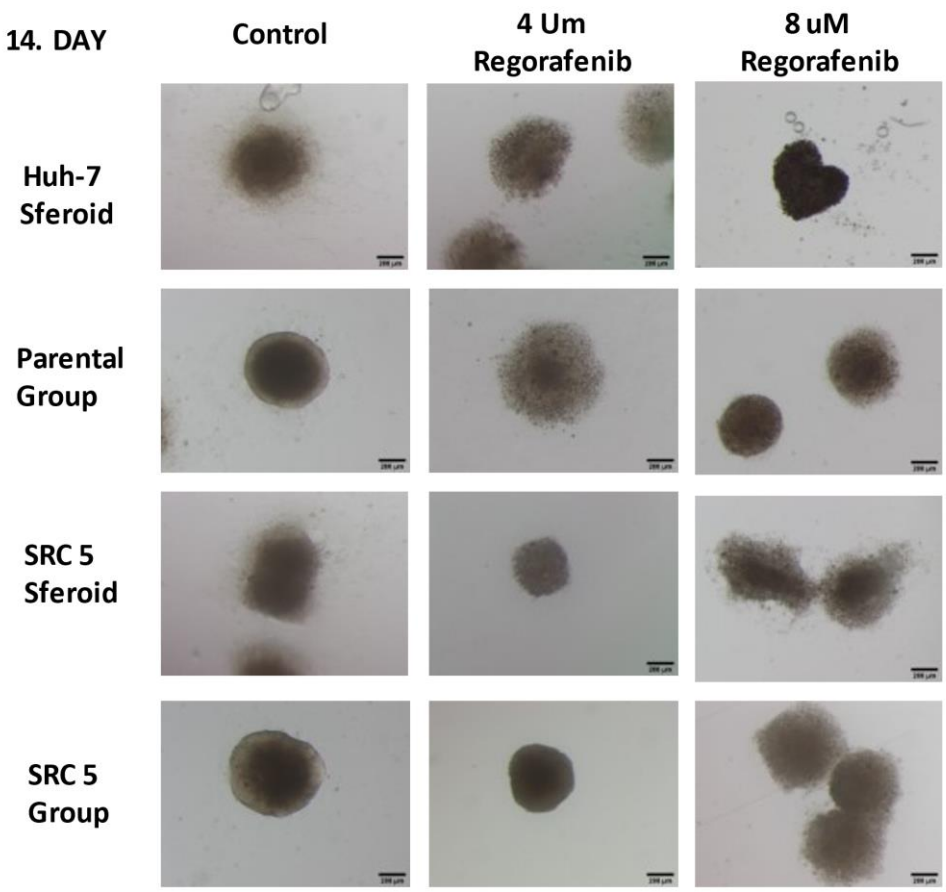

Figure 16. Parental (Huh7+LX-2 cells) and SRC5 (SRC5+LX-2) spheroids were treated with Regorafenib for 7 days in the poly-HEMA coated plates and were visualized under the light microscope on the 14th day of culture.

4.2.4 Labeling of cells using lentiviral plasmids

To visualize HCC and microenvironment cells separately, cells were transfected with lentiviral plasmids carrying fluorescent tags with different colors. Huh7 and sorafenib resistant clone SRC cells were transfected with mCherry (red), LX-2 cells with Azurre (blue) and THP-1 cells with GFP (green). Spheroids were formed using transfected cells and visualized (Figure 17).

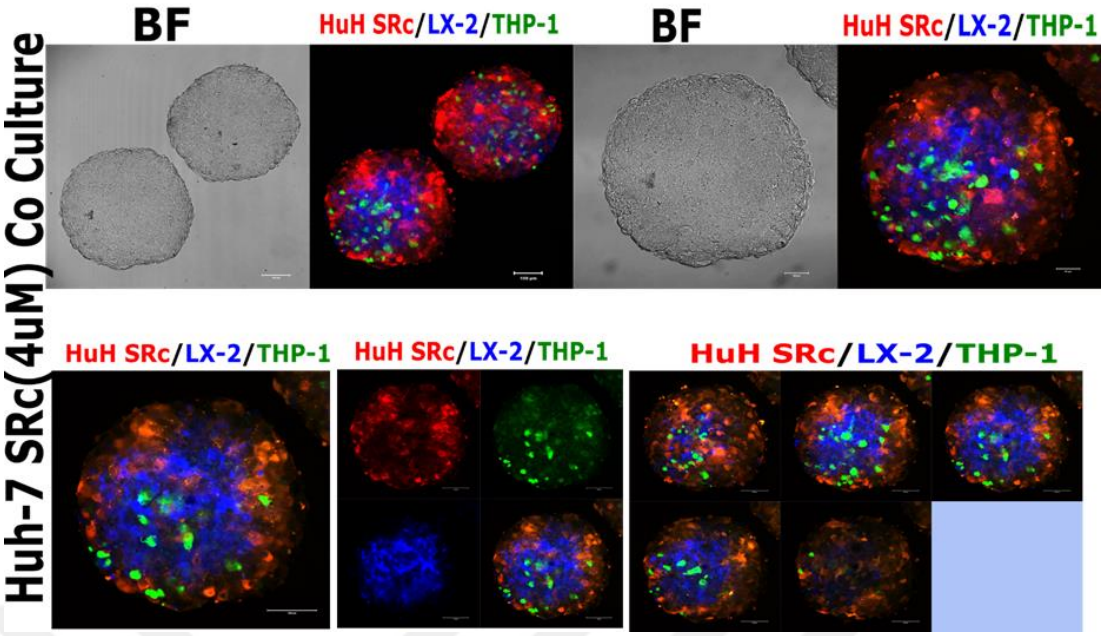

Figure 17. Transfected SRC5 (SRC5+LX-2+THP-1) spheroids were visualized under confocal microscopy. Red: SRC-mCherry, Blue: LX2-Azurete, Green: THP1-GFP.

4.3 Analysis of Spheroids

4.3.1 Cell proliferation and viability

4.3.1.1. Ki67 Staining

Ki67 staining was performed for proliferation analysis. Expression of the Ki67 protein is associated with the proliferative activity tumors, it is used as a marker of tumor aggressiveness. Both parental and SRC spheroids demonstrated a high number of proliferative cells (Figure 18).

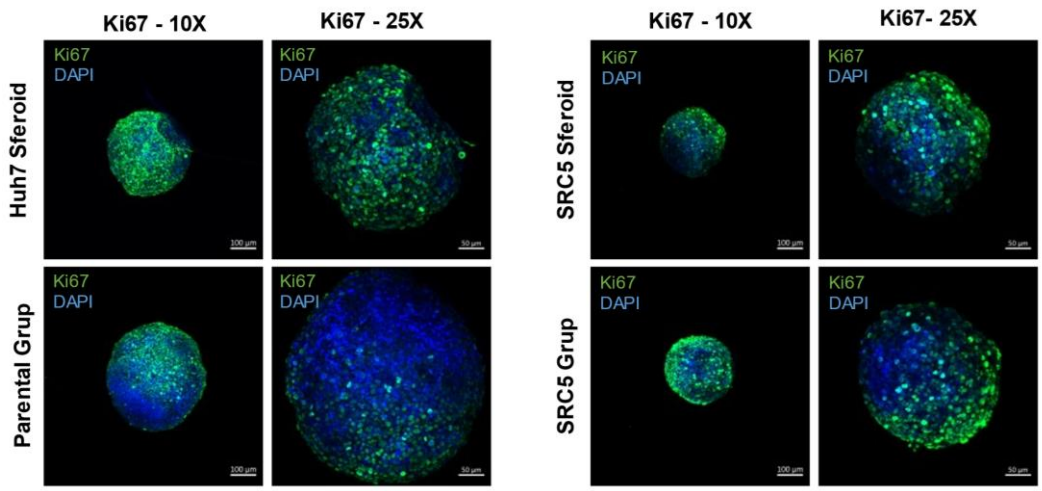

Figure 18. Ki67 staining was performed with parental (Huh7+LX-2 cells) and SRC5 (SRC5+LX-2) spheroids.

4.3.1.2. Viability Analysis

Calcein AM and PI staining were performed for viability analysis. Calcein AM is a cell membrane permeable dye and gives a green fluorescent glow after hydrolysis by intracellular esterases. PI, on the other hand, cannot pass through the membrane of living cells, so it is used to stain cell membrane-damaged necrotic or late apoptosis/dead cells. Both parental and SRC spheroids demonstrated a high number of live cells (Figure 19).

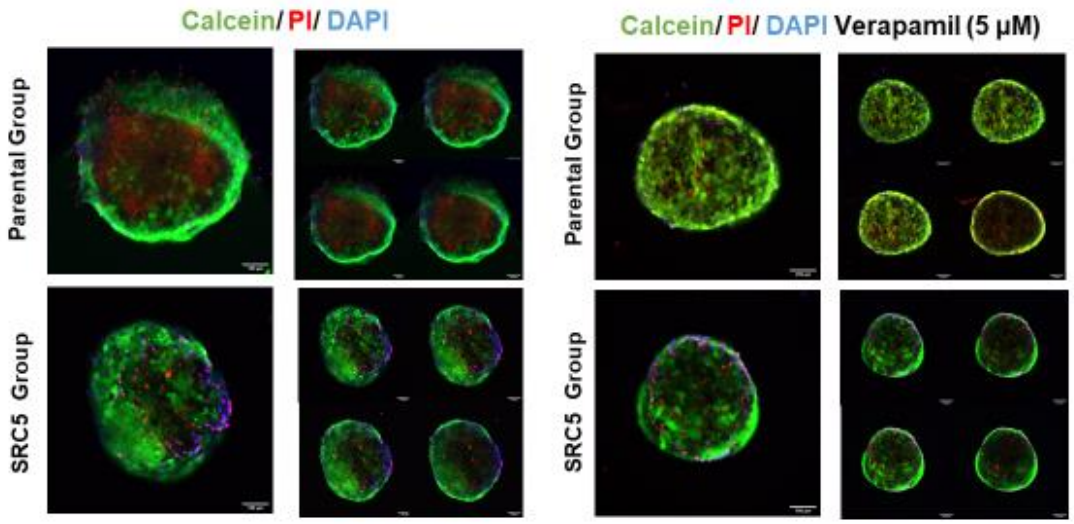

Figure 19. Calcein AM and PI staining was performed with parental (Huh7+LX-2+THP-1 cells) and SRC5 (SRC5+LX-2+THP-1 cells) spheroids.

4.3.2. Analysis of f-actin by Phalloidin Staining

To examine the spheroid structure, f-actin staining was performed using phalloidin. Phalloidin staining also showed that Sorafenib-resistant SRC5 spheroids had a different f-actin organization than parental spheroids (Figure 20).

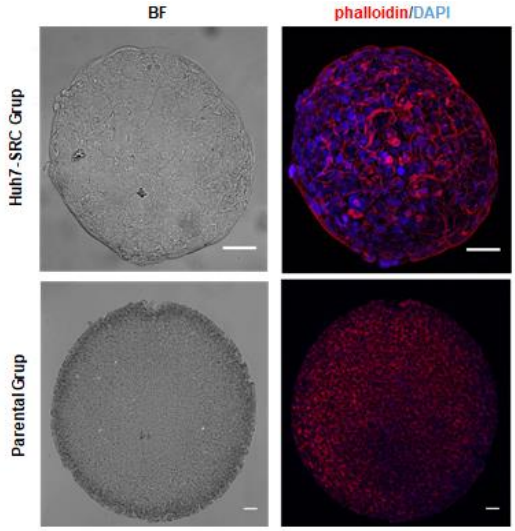

Figure 20. Phalloidin staining parental (Huh7+LX-2+THP-1 cells) and SRC5 (SRC5+LX-2+THP-1 cells) spheroids.

4.3.3. Analysis of E-cadherin and β-integrin Expression

Cell-cell and cell-matrix interactions were analysed by E-cadherin and β1-integrin staining. SRC spheroids also demonstrated a different pattern of E-cadherin and β1-integrin staining compared to parental spheroids (Figure 21-22).

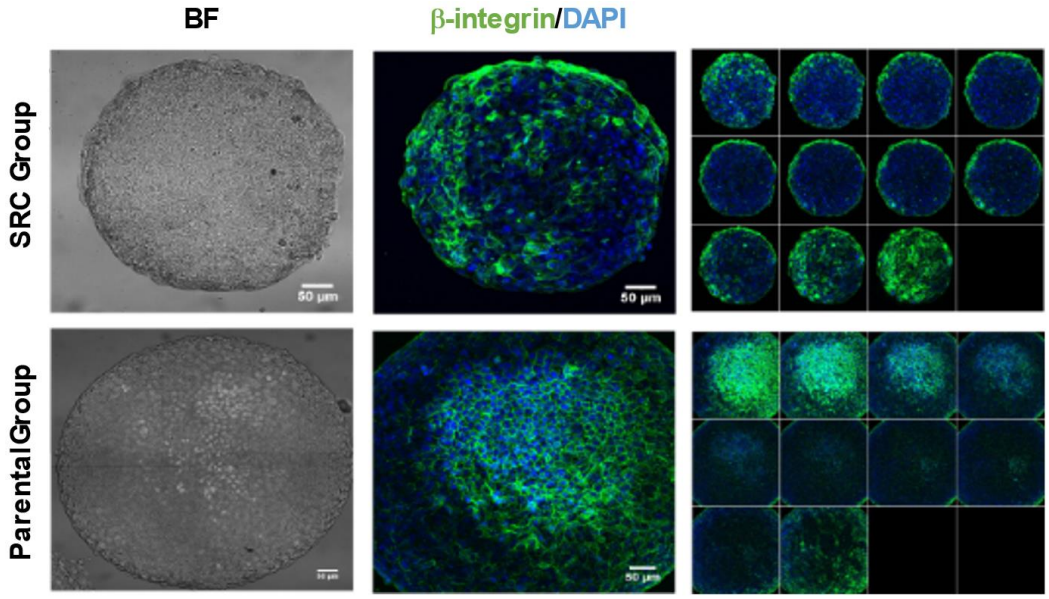

Figure 21. β−integrin staining was performed with parental (Huh7+LX-2+THP-1 cells) and SRC5 (SRC5+LX-2+THP-1 cells) spheroids.

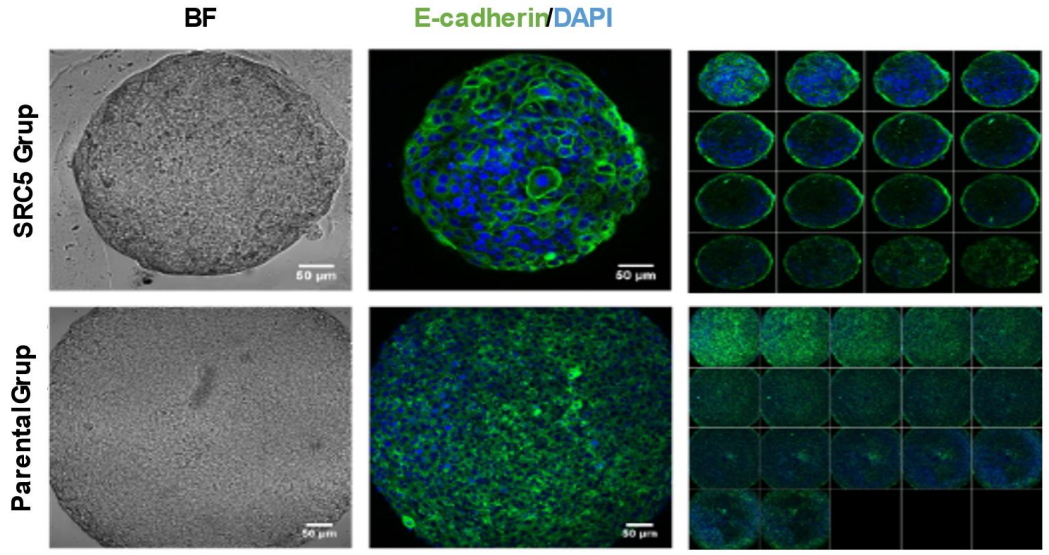

Figure 22. E-cadherin staining was performed with parental (Huh7+LX-2+THP-1 cells) and SRC5 (SRC5+LX-2+THP-1 cells) spheroids.

4.3.4 Analysis of MDR1 Expression

4.4.4.1. MDR1 Staining on Basal Spheroids

MDR (Multidrug resistance) is a transporter that promotes failure of cancer treatment by overexpressing ABC (ATP-binding cassette) transporters to decrease

drug efficiency. MDR1 staining was performed on basal spheroids to detect MDR1 expression. There was no significant difference in MDR expression of spheroids (Figure 23).

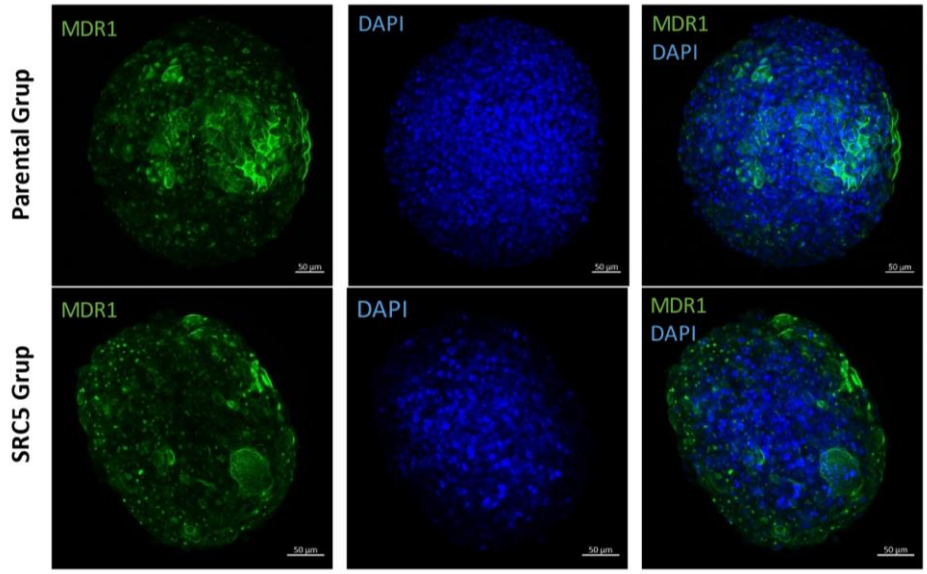

Figure 23. MDR1 staining was performed with parental (Huh7+LX-2 cells) and SRC5 (SRC5+LX-2 cells) spheroids.

4.4.4.2. MDR1 Staining with Control and Regorafenib Treatment Transfected Spheroids

We also used transfected cells in order to see MDR1 expression in different cell types. In both parental and SRC spheroids MDR1 expression is associated with HCC cells. After regorafenib treatment while Huh7 cells in parental spheroids are greatly lost, thus the MDR1 expression. On the other hand in SRC spheroids, after regorafenib treatment the number of Huh7-SRC cells and the amount of MDR-1 expression still stays high (Figure 24).

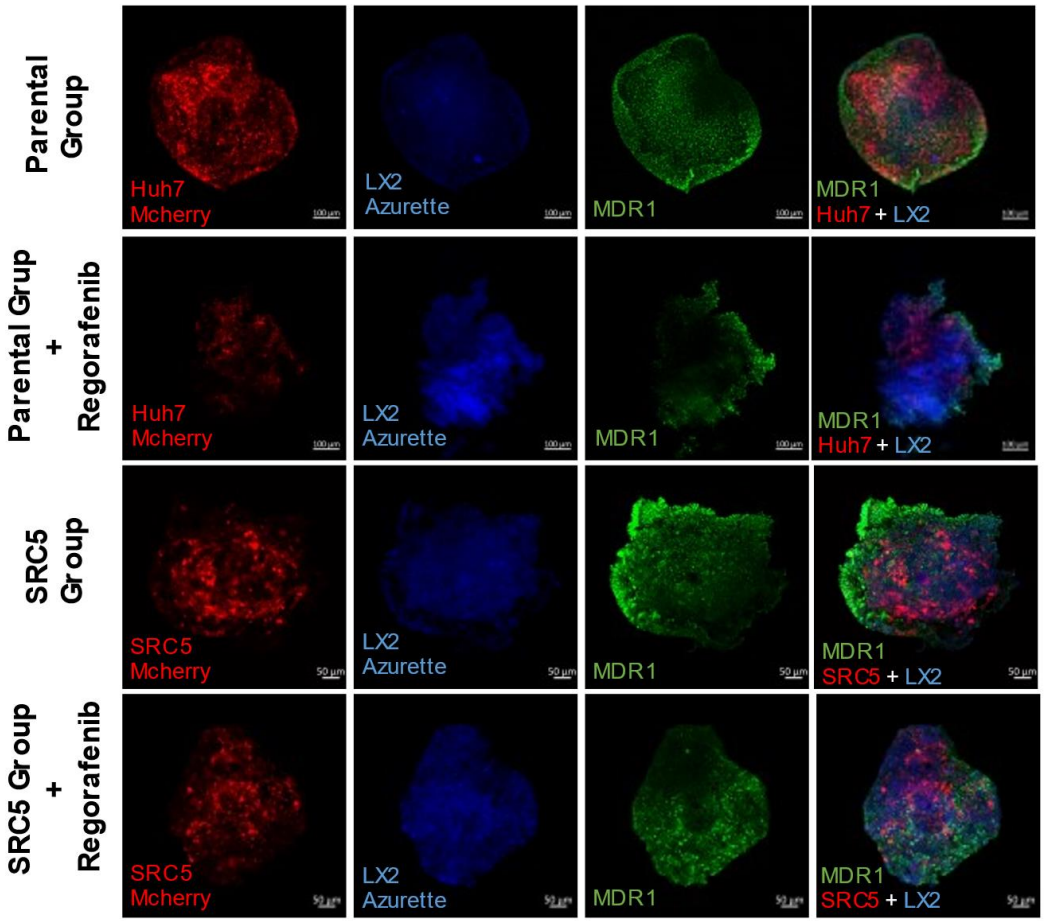

Figure 24. MDR staining was performed with transfected parental (Huh7-mCherry+LX-2-Azzure cells) and transfected SRC5 (SRC5- mCherry+LX-2-Azzure cells) spheroids.

4.4. Analysis of TME Activation

4.4.1 Alpha-sma Staining of Activated LX-2 Cells

In this experiment, it was aimed to determine the activation states of microenvironment (LX-2) cells in Huh7 Parental and SRC sorafenib resistant spheroids. α-sma protein was chosen as a marker for the activation of LX-2 cells.

Immunostainings were first tested in classical 2-D cell culture using positive controls. As a positive control, LX-2 cells were incubated with 1 ng/ml TGF-β for 24 hours. While α-sma expression was very low in control LX-2 cells, a large increase in α-sma expression was observed as a result of TGF-β treatment. This indicates that LX-2 cells are activated upon TGF-β treatment (Figure 25).

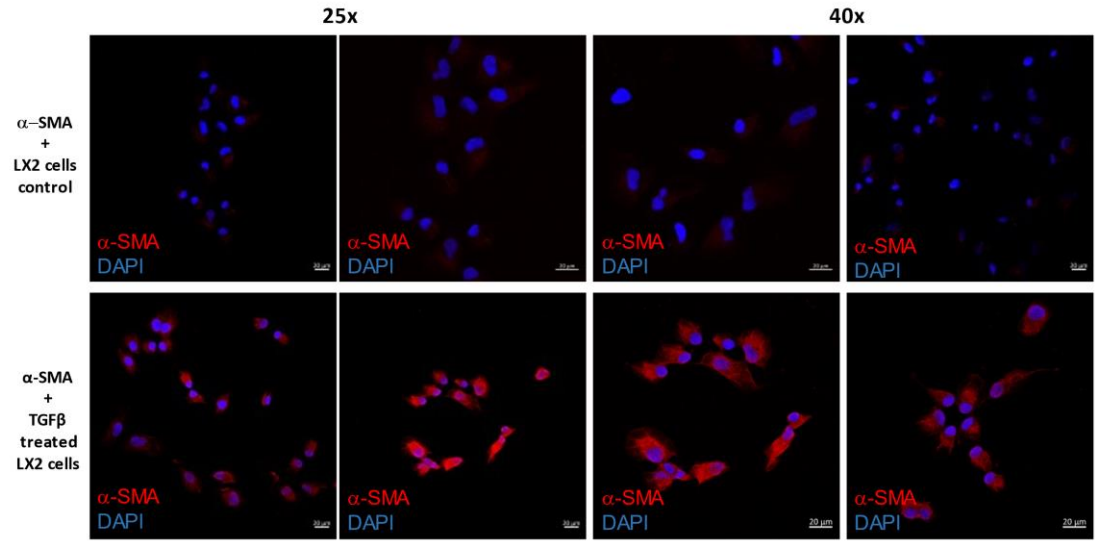

Figure 25. Immunofluorescent analysis of activated LX-2 cells using α-sma antibody. Red-α-sma, blue- DAPI.

α-sma staining was tested on 3-D spheroids to determine basal activation states in parental and SRC spheroids. Confocal microscope examinations detected α-SMA staining in SRC spheroids, indicating that LX-2 cells in SRC spheroids were activated (Figure 26).

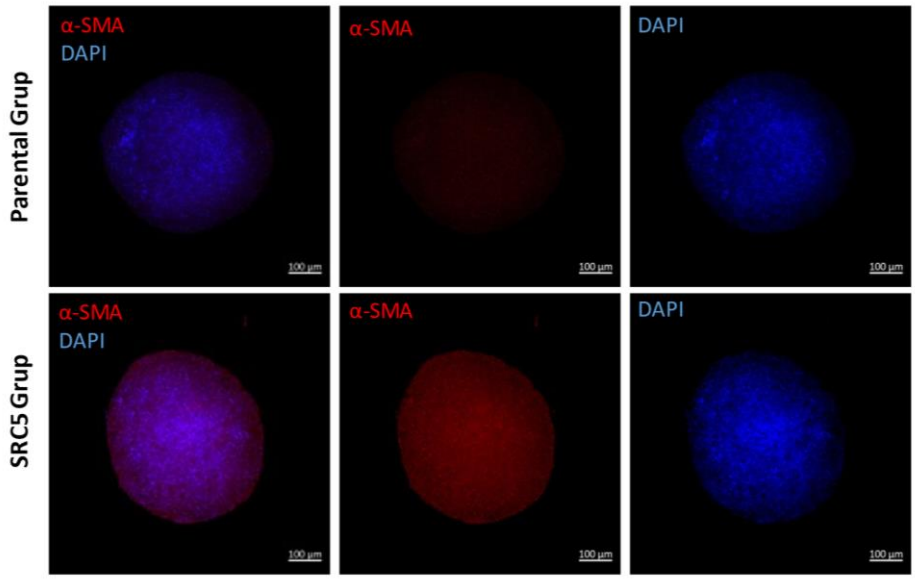

Figure 26. α−sma staining was performed with Parental (Huh7+LX-2 cells) and SRC5 (SRC5+LX-2 cells) Spheroids. Red-α-sma, blue- DAPI.

4.4.2 Analysis of ECM production in Spheroids

4.4.2.1 Collagen I and Laminin Staining

Collagen 1 and Laminin stainings were performed to determine if there was increased ECM secretion as a result of LX-2 activation. As a result of confocal analysis, more Laminin was detected in Huh7 parental and SRC spheroids formed with LX-2 cells compared to spheroids formed with a single cell group. In addition, the amount of Collagen 1 was increased in SRC spheroids (Figure 27-28).

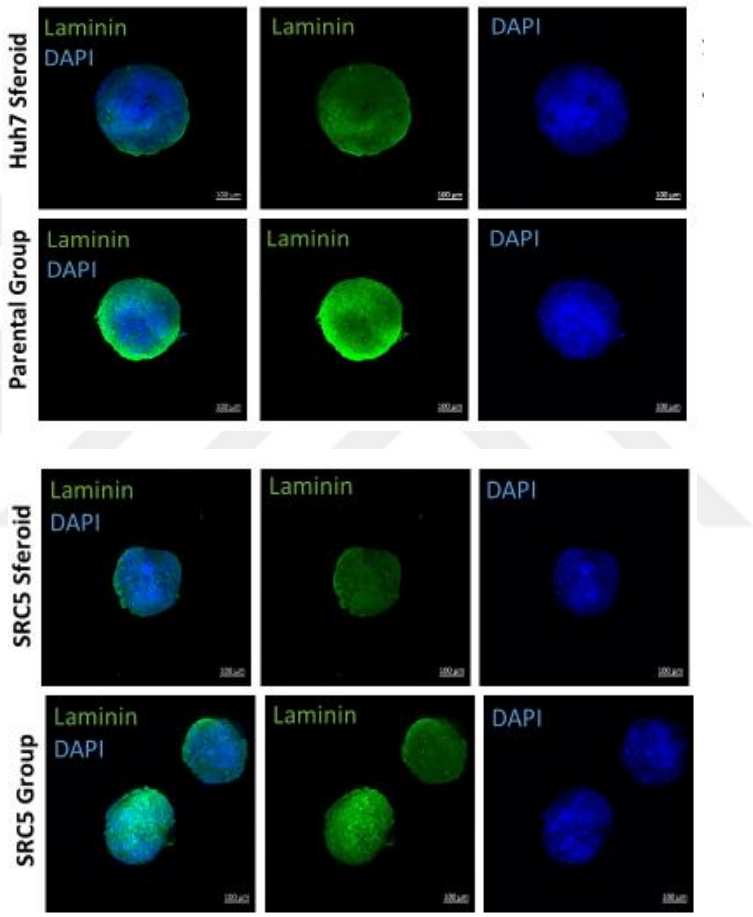

Figure 27. Laminin staining was performed with Huh7 only, Parental (Huh7+LX-2 cells), SRC5 only and, SRC5 (SRC5+LX-2 cells) Spheroids.

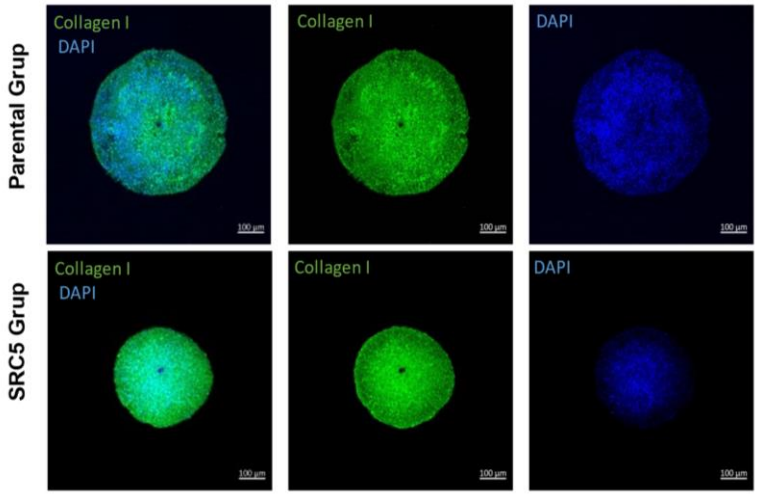

Figure 28. Collagen 1 staining was performed with Parental (Huh7+LX-2 cells) and SRC5 (SRC5+LX-2 cells) spheroids.

4.4.3 Immunofluorescent Analysis of Activated THP-1 Cells

In this experiment, it was aimed to determine the activation states of THP-1 cells in Huh7 Parental and SRC spheroids. CD68 protein was chosen as a marker for the activation of THP-1 cells. THP1 cells treated with Phorbol-12-Myristate-13-Acetate (PMA) were used for positive control. THP1 monocyte cells growing in suspension were treated with 150 nM PMA for 48 hours to allow cells to differentiate into macrophages. Control THP-1 cells that were not stimulated with PMA continued to grow in a round shape and suspended form without adhering to the plastic surfaces of the culture plates, whereas THP1 cells differentiated by PMA treatment flattened and adhered to the plastic surfaces of the culture plates. These adherent cells also showed increased CD68 expression in the cytoplasm and membrane (Figure 29).

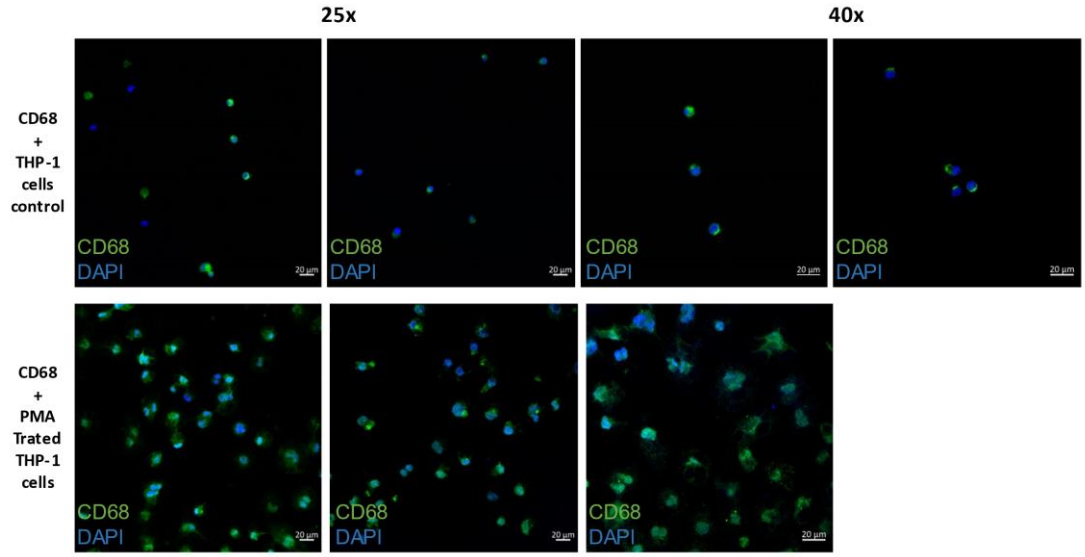

Figure 29. Immunofluorescent analysis of activated THP-1 cells with CD68 and DAPI.

CD68 staining in 3-D spheroids gave high background staining due to the density of THP1 cells in both parental and SRC spheroids. However, their confocal images showed a lower and more punctual CD68 staining in parental THP1 cells than in control THP1 cells, whereas THP1 cells in SRC spheroids showed higher and diffuse CD68 expression (Figure 30).

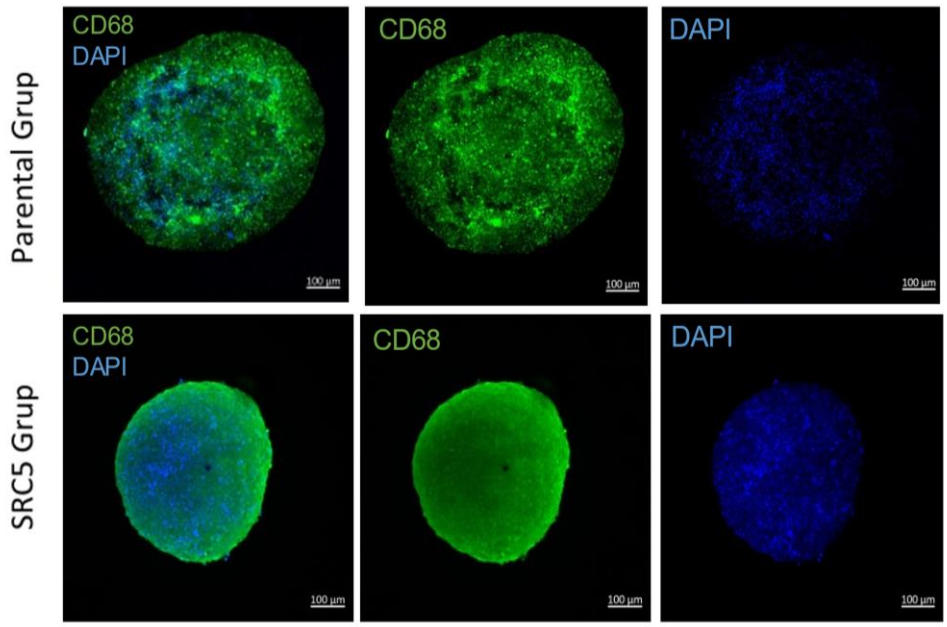

Figure 30. CD68 staining was performed with Parental (Huh7+LX-2 cells) and SRC5 (SRC5+LX-2 cells) spheroids.

4.5. Analysis of Cancer Stem Cell Marker Expression

We aimed to analyse stem cell markers by flow cytometry. EpCAM, CD133 and CD24 membrane proteins were used for this experiment. The flow cytometer analysis demonstrated that CD24+ and EpCAM+ stem cell population was increased in sorafenib resistant spheroids (Figure 31).

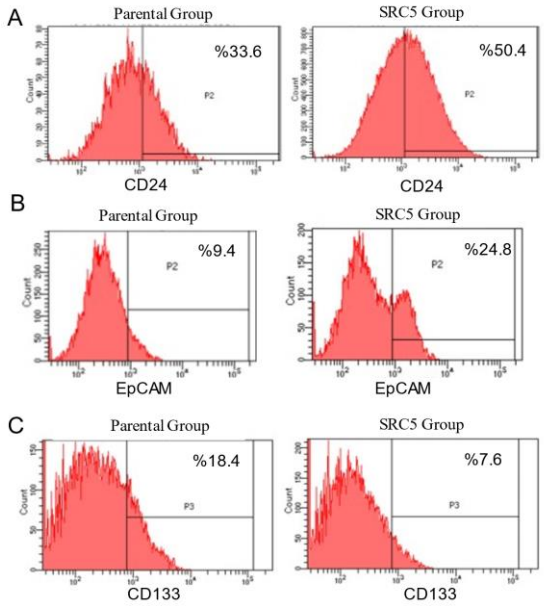

Figure 31. Stem-cell marker expression (CD24+, EpCAM+ and CD133+) was analyzed in Parental (Huh7 + LX-2) and SRC (SRC5+LX-2) Spheroids.

4.6 Cytokine Array and Kinase Array

We aimed to determine the differences in terms of cytokine secretion and activated kinases in parental and SRC spheroids. For this, we analyzed the conditioned medium of spheroids incubated for 16 hours in 1% FBS medium for the determination of cytokines. To analyse 105 cytokines simultaneously, a cytokine array (R&D Systems, ARY022B, Table 1) containing antibodies dotted on a nitrocellulose membrane was used as specified in the instruction manual. Briefly, the medium collected from the spheroids was placed on the nitrocellulose membrane that was previously blocked for 1 hour and incubated at +4oC overnight. Detection and analysis were then performed as described above. The first analysis was performed using the density reference points and the image analysis program (Figure 32).

Adiponectin/Acrp30	IFN-gamma	CCL2/MCP-1
Angiogenin	IGFBP-2	CCL7/MCP-3
Angiopoietin-1	IGFBP-3	M-CSF
Angiopoietin-2	IL-1 alpha/IL-1F1	MIF
Apolipoprotein A1	IL-1 beta/IL-1F2	CXCL9/MIG
BAFF/BLyS/TNFSF13B	IL-1ra/IL-1F3	CCL3/CCL4 MIP-1 alpha/beta
BDNF	IL-2	CCL20/MIP-3 alpha
CD14	IL-3	CCL19/MIP-3 beta
CD30	IL-4	MMP-9
CD31/PECAM-1	IL-5	Myeloperoxidase
CD40 Ligand/TNFSF5	IL-6	Osteopontin (OPN)
Chitinase 3-like	IL-8	PDGF-AA
Complement Component C5/C5a	IL-10	PDGF-AB/BB
Complement Factor D	IL-11	Pentraxin 3/TSF-14
C-Reactive Protein/CRP	IL-12 p70	CXCL4/PF4
Cripto-1	IL-13	RAGE
Cystatin C	IL-15	CCL5/RANTES
Dkk-1	IL-16	RBP4
DPPIV/CD26	IL-17A	Relaxin-2
EGF	IL-18 BPa	Resistin
CXCL5/ENA-78	IL-19	CXCL12/SDF-1 alpha
Endoglin/CD105	IL-22	Serpin E1/PAI-1
EMMPRIN	IL-23	SHBG
Fas Ligand	IL-24	ST2/IL1 R4
FGF basic	IL-27	CCL17/TARC
KGF/FGF-7	IL-31	TFF3
FGF-19	IL-32 alpha/beta/gamma	TfR
Flt-3 Ligand	IL-33	TGF-alpha
G-CSF	IL-34	Thrombospondin-1
GDF-15	CXCL10/IP-10	TIM-1
GM-CSF	CXCL11/I-TAC	TNF-alpha
CXCL1/GRO alpha	Kallikrein 3/PSA	uPAR
Growth Hormone (GH)	Leptin	VCAM-1
HGF	LIF	VEGF
ICAM-1/CD54	Lipocalin-2/NGAL	Vitamin D BP

Figure 32. Cytokines detectable with the Human XL Cytokine Array (R&D Systems, ARY022B)

For the kinase array, the spheroids were immediately washed with 1XPBS after the medium was taken, and lysates were prepared using the lysis buffer provided in

the kit after the addition of protease and phosphatase inhibitors. The lysates were then incubated at +4oC overnight on the nitrocellulose membranes contained in the Human Phospho-kinase assay (R&D Systems, ARY003C, Table 2) kit. Detection and analysis were then performed as described above (Fig. 33).

Simultaneously detect the relative phosphorylation of these proteins in a single sample.		
Akt 1/2/3 (S473)	HSP60	PRAS40 (T246)
Akt 1/2/3 (T308)	JNK 1/2/3 (T183/Y185, T221/Y223)	Pyk2 (Y402)
beta-Catenin	Lck (Y394)	RSK1/2 (S221/S227)
Chk-2 (T68)	Lyn (Y397)	RSK1/2/3 (S380/S386/S377)
c-Jun (S63)	MSK1/2 (S376/S360)	Src (Y419)
CREB (S133)	p38 alpha (T180/Y182)	STAT1 (Y701)
EGF R (Y1086)	p53 (S15)	STAT2 (Y689)
eNOS (S1177)	p53 (S392)	STAT3 (S727)
ERK1/2 (T202/Y204, T185/Y187)	p53 (S46)	STAT3 (Y705)
Fgr (Y412)	P70 S6 Kinase (T389)	STAT5a/b (Y699)
GSK-3 alpha/beta (S21/S9)	p70 S6 Kinase (T421/S424)	STAT6 (Y641)
GSK-3 beta (S9)	PDGF R beta (Y751)	WNK-1 (T60)
HSP27 (S78/S82)	PLC gamma-1 (Y783)	Yes (Y426)

Figure 33. Kinases detectable by the Human Phospho-Kinase Assay (R&D Systems, ARY003C).

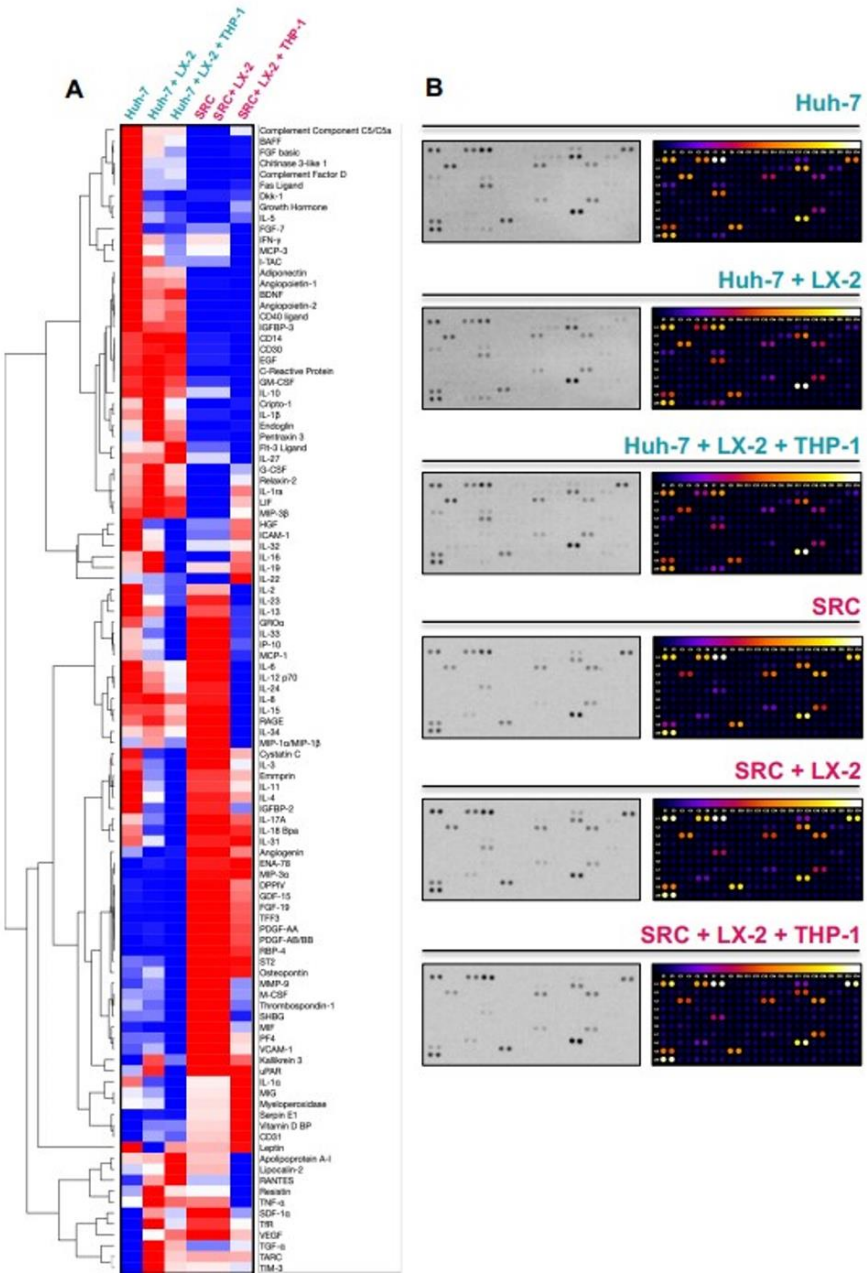

Figure 34. Cytokine profiles of Parental and Sorafenib resistant 3-D tumor spheroids. A. Heatmap reflecting cytokine expression by hierarchical cluster analysis. B. Cytokine array membrane (left) and pixel density analysis (right). Protein Array Analyzer (ImageJ) (Carpantier and Henault, 2010) was used for pixel density analysis, and Morpheus software (Broad Institute) was used for hierarchical cluster analysis and heat map creation. In hierarchical clustering analysis, the distances between genes was calculated by 1-Pearson Correlation, the mean was used as the linkage method, and the clusters were constructed as row (gene)-based.

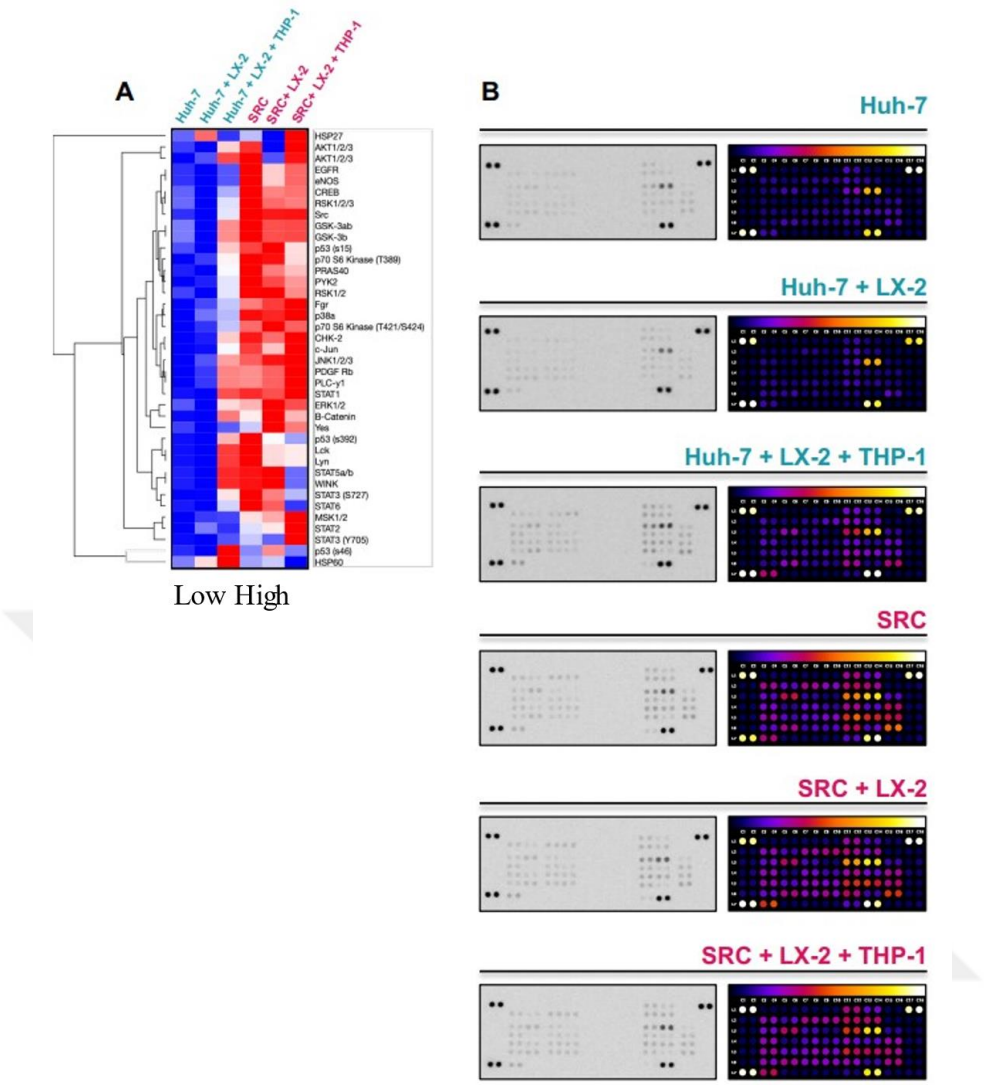

Figure 35. Kinase profiles of Parental and Sorafenib resistant 3-D tumor spheroids. A. Heatmap reflecting kinase expression after hierarchical cluster analysis. B. Kinase array membrane (left) and pixel density analysis (right). Protein Array Analyzer (ImageJ) was used for pixel density analysis, and Morpheus software (Broad Institute) was used for hierarchical cluster analysis and heat map creation. In hierarchical clustering analysis, the distance between genes was calculated by 1-Pearson Correlation, the mean was used as the linkage method, and the clusters were constructed as row (gene)-based.

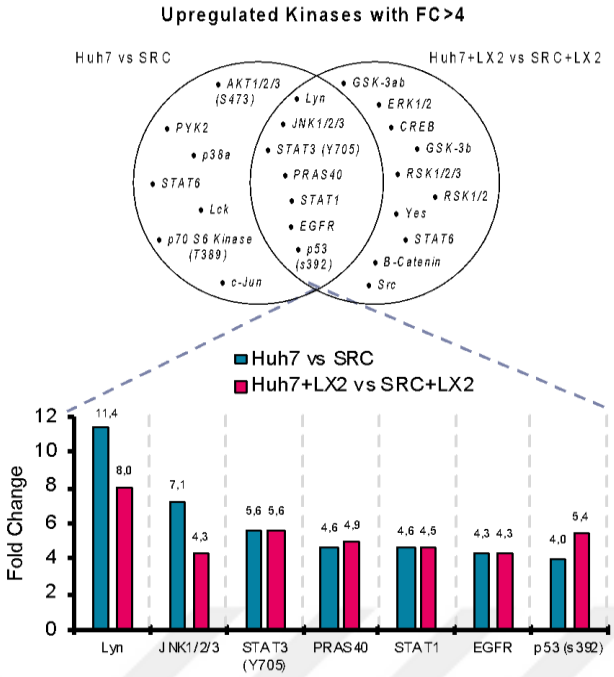

Figure 36. Differential kinase expression of Huh7 vs SRC5 and Huh7+LX-2 vs SRC5+LX-2 spheroids.

The results of the cytokine array showed that compared to Huh7 only spheroids, spheroids formed with 3 cell types had an increased in the secretion of IFN-γ, MCP-3, FGF-7, FGF Basic, Dkk-1, Fas Ligand and IL-5. In SRC spheroids when LX-2 and THP1 cells are present, there was a higher activation of IL-1a, MIG, Myeloperoxide, Serpin E1, Vitamin D BD, CD31 and Leptin. When comparing the SRC spheroids and SRC+LX-2 spheroids to Huh7 spheroids and Huh7+LX-2 spheroids, there was a higher activation of IL-3, IL-11, IL-4, IGFBP-2, IL-17A, Angiogenin, PDGF-AA, PDGF-AB/BB, RBP-4, MMP-9.

The results of the kinase array showed that compared to Huh7 spheroids, in SRC spheroids, there was higher activation of AKT 1/2/3, p38a, Lck, STAT6 and other kinases shown in Figure 35. When comparing SRC+LX-2 spheroids to Huh7+LX-2 spheroids, there was a higher activation of GSK-3 ab, ERK 1/2, GSK-3b and other kinases shown in Figure 35. Moreover, Lyn, JNK1/2/3, STAT 3, PRAS 40, STAT1, EGFR and p53 (s392) both showed higher activation in SRC spheroids and SRC+LX-2 spheroids when compared to Huh7 spheroids and Huh7+LX-2 spheroids.

CHAPTER 5: DISCUSSION

The pre-clinical studies evaluating the efficacy and cytotoxicity of cancer treatment drugs such as sorafenib and regorafenib are vital before treatment in the clinic. However, *in vitro* drug studies are commonly based on 2D cultures and 2D cultures are not successful enough to mimic tumor microenvironment. In this thesis, parental and sorafenib resistant 3D HCC tumor spheroids were generated using 3D hanging drop method. These models offer similarities to tumor microenvironment in terms of cell-cell communications, extracellular matrix interaction and oxygen and nutrient gradient. Thus, drug studies done using 3D models produce results that can better translate into clinic and thus are more valuable.

To our knowledge, there is no 3D model with sorafenib resistant cells in the literature. In this thesis, we developed a sorafenib resistant model that demonstrated high cell survivals and they had large diameter and acceptable growth area. When we compared parental spheroids with sorafenib resistant spheroids, immunosuppression was increased in the sorafenib resistant spheroids because of higher IL-8 levels, also, sorafenib resistant spheroids showed higher tumor-related genes and liver-related genes (β-catenin, p53, Lyn, STAT, EGFR, VEGF, PDGF-AA and PDGF-AB/BB) that take part in metastasis, proliferation, drug resistance, immunosuppression and epithelial to mesenchymal transition of tumor cells. The stem cell markers such as EpCAM and CD24 were also found at higher levels in sorafenib resistant spheroids which indicated that sorafenib resistant tumors have higher potential for invasion, metastasis and recurrence compared to parental spheroids.

Immune-checkpoint inhibitors (ICIs) have been approved as second-line or first-line therapies for a list of malignancies including liver cancer (Gong et al., 2018). However, tumor response rates for these ICIs are low, being less than 20% in HCC (El-Khoueiry A.B. et al., 2017), (Zhu, A. X. et al., 2018), (Sangro, B. et al., 2013). The highly immunosuppressive tumor environment in advanced HCC is believed to contribute to low treatment response of HCC to ICIs (Prieto, J. et al., 2015). Our results also suggest that sorafenib resistant tumors have a different immune signature than parental spheroids and our model can be used to investigate the effect of new therapies such as ICIs.

CHAPTER 6: CONCLUSION

We aimed to develop parental and sorafenib resistant SRC spheroid models that can mimic tumor environment in order to better analyse how sorafenib-resistant cells will respond to regorafenib treatment. First, MTT analysis of the Huh7 parental cell line and its sorafenib resistant clone was performed using both sorafenib and regorafenib. According to the results, SRC clone was highly resistant to sorafenib. Also, the IC50 value of SRC clone was higher than parental clone for regorafenib. This demonstrated that sorafenib resistant cells also acquired Regorafenib resistance. It supports the main argument of this thesis.

We decided to co-culture three cell types (Huh7, LX-2 and THP-1). Optimization experiments were carried out to determine how much of each cell line to use and percentages of cell populations. When the optimization experiments were done, we wanted to analyse the effect of regorafenib on parental and sorafenib resistant spheroids. In this process, spheroids were collected from hanging droplets on the 7th day and dispensed into poly-HEMA coated plates and treated with 4 micromolar regorafenib. Our results demonstrated that SRC spheroids are also more resistant to regorafenib than parental spheroids.

Calcein AM/ PI staining and Ki67 staining was performed for viability and for proliferation analysis. Both parental and SRC spheroids demonstrated a high number of proliferative cells and demonstrated high viability. To understand the spheroid structure, f-actin staining was performed using phalloidin. It showed that Sorafenib-resistant SRC5 spheroids had a different f-actin organization than parental spheroids. Cell-cell and cell-matrix interactions were analysed by E-cadherin and β1-integrin staining, respectively. Compared to parental spheroids, SRC spheroids also demonstrated a different staining pattern for both E-cadherin and β1-integrin expressions.

We also transfected cells with lentiviral plasmids carrying fluorescent tags with different colors (Huh7 cells and sorafenib resistant clone SRC cells (mCherry (red)), LX-2 cells (Azurre (blue)) and THP-1 cells (GFP (green)) and generated parental and sorafenib resistant SRC spheroids. By this method, we were able to visualize HCC and microenvironment cells separately. We performed MDR1 staining on these spheroids. Although basal MDR1 expression seemed similar, after regorafenib treatment while Huh7 cells in parental spheroids were greatly lost, in SRC spheroids the number of

Huh7-SRC cells and the amount of MDR-1 expression still stayed high. Moreover, flow cytometry analysis of cancer stem cell markers showed that CD24+ and EpCAM+ stem cell population was increased in sorafenib resistant spheroids demonstrating that the SRC spheroids have a higher cancer stem cell population than parental spheroids.

In order to determine the activation states of microenvironment (LX-2) cells in Huh7 Parental and SRC sorafenib resistant spheroids, we evaluated the expression of α-sma protein. While α-sma expression was very low in control LX-2 cells, a large increase in α-sma expression was observed as a result of TGF-β treatment. This indicates that LX-2 cells are activated upon TGF-β treatment. α-sma staining was tested on 3-D spheroids to determine basal activation states in parental and SRC spheroids. Confocal microscope imaging detected α-SMA staining in SRC spheroids, indicating that LX-2 cells in SRC spheroids were activated. Collagen 1 and Laminin stainings were also performed to analyse ECM productions in spheroids. Confocal image analysis demonstrated that there was more Laminin in both Huh7 parental and SRC spheroids formed with LX-2 cells compared to spheroids formed with a single cell group. In addition, the amount of Collagen 1 was increased in SRC spheroids, again indicating LX-2 activation.

In order to determine the activation states of THP-1 cells in Huh7 Parental and SRC spheroids, CD68 protein expression was evaluated. As a positive control, THP-1 cells were treated with PMA. PMA induced THP-1 cells became adherent and demonstrated increased CD68 expression in the cytoplasm and membrane. When we performed this staining in 3-D spheroids, CD68 staining gave high background due to the density of THP1 cells in both parental and SRC spheroids. However, confocal images showed a lower and more punctual CD68 staining in THP1 cells in parental spheroids, whereas THP1 cells in SRC spheroids showed higher and diffuse CD68 expression similar to CD68 in activated monocytes.

In addition, we determined the differences in terms of cytokine secretion and activated kinases in parental and SRC spheroids. The results of the cytokine array showed that compared to Huh7 only spheroids, spheroids formed with 3 cell types had an increase in the secretion of IFN-γ, MCP-3, FGF-7 and other cytokines shown in Figure 32. In SRC spheroids when LX-2 and THP1 cells were present, there was a higher activation of IL-1a, MIG, Myeloperoxide and others shown in Figure 32. Moreover, in SRC spheroids when LX-2 and THP1 cells were present, there was a

higher activation of kinases such as Lyn, EGFR, PDGFR and other kinases shown in Figure 34. According to results, there are high enzyme linked receptor protein signalling, transmembrane receptor protein tyrosine kinase signalling pathway and receptor signalling pathway via JAK-STAT in SRC spheroids.

In conclusion, our 3-D spheroid model represents a feasible, reproducible and cheaper cell-culture model in which many cell types can be co-cultured together without a need for adherence. These cells secrete their own ECM and form tumor spheroids with high viability and active signalling. In this model, we investigated sorafenib resistant cells. Our results clearly demonstrate that SRC spheroids are different from parental spheroids in terms of cytoskeletal organization, cell-cell and cell-matrix interactions, ECM composition and cancer stem cell population. Moreover, parental and sorafenib resistant SRC spheroids show different regorafenib responses and their interaction with LX-2 and THP1 cells differ. While SRC spheroids are more regorafenib resistant, they also have activated LX-2 and THP1 cells. Our results indicate the importance of including microenvironment cells in cancer research. The 3-D spheroid model established in this thesis offers a cell-culture system for mimicking the tumor microenvironment using multiple cell types which would be beneficial in various stages of cancer research including drug screening and development.

REFERENCES

Abbott, A. (2003) '*Biology's new dimension'*, Nature, pp. 870–872.

Abou-Alfa, G. K., Meyer, T., Cheng, A. L., El-Khoueiry, A. B., Rimassa, L., Ryoo, B. Y., Cicin, I., Merle, P., Chen, Y., Park, J. W., Blanc, J. F., Bolondi, L., Klümpen, H. J., Chan, S. L., Zagonel, V., Pressiani, T., Ryu, M. H., Venook, A. P., Hessel, C., Borgman-Hagey, A. E., Kelley, R. K. (2018) *Cabozantinib in patients with advanced and progressing hepatocellular carcinoma*, The New England journal of medicine, 379(1), 54–63.

Asai, R., Tsuchiya, H., Amisaki, M., Makimoto, K., Takenaga, A., Sakabe, T., Hoi, S., Koyama, S., & Shiota, G. (2019) *CD44 standard isoform is involved in maintenance of cancer stem cells of a hepatocellular carcinoma cell line*, Cancer medicine, 8(2), 773–782.

Bhatia, A. and Kumar, Y. (2020) *Cancer immunoediting: Immunosurveillance, immune equilibrium, and immune escape*, in Cancer Immunology: A Translational Medicine Context, Second Edition. Springer International Publishing, pp. 291–305.

Birgani, M. T. and Carloni, V. (2017) *Tumor microenvironment, a paradigm in hepatocellular carcinoma progression and therapy*, International Journal of Molecular Sciences, 18(2), pp. 7–10.

Bourguignon, L. Y. W., Shiina, M. and Li, J. J. (2014) *Hyaluronan-CD44 interaction promotes oncogenic signaling, microRNA functions, chemoresistance, and radiation resistance in cancer stem cells leading to tumor progression*, in Advances in Cancer Research. Academic Press Inc., pp. 255–275.

Calcagno, A. M., Kim, I. W., Wu, C. P., Shukla, S., & Ambudkar, S. V. (2007*) ABC drug transporters as molecular targets for the prevention of multidrug resistance and drug-drug interactions*, Current drug delivery, 4(4), 324–333.

Calcagno, A. M., Salcido, C. D., Gillet, J. P., Wu, C. P., Fostel, J. M., Mumau, M. D., Gottesman, M. M., Varticovski, L., & Ambudkar, S. V. (2010) *Prolonged drug selection of breast cancer cells and enrichment of cancer stem cell characteristics*, Journal of the National Cancer Institute, 102(21), 1637–1652.

Cekanova, M. and Rathore, K. (2014) *Animal models and therapeutic molecular targets of cancer: Utility and limitations*, Drug Design, Development and Therapy. Dove Medical Press Ltd., pp. 1911–1922.

Chen, G. G., Merchant, J. L., Lai, P. B., Ho, R. L., Hu, X., Okada, M., Huang, S. F.,

Chui, A. K., Law, D. J., Li, Y. G., Lau, W. Y., & Li, A. K. (2003) *Mutation of p53 in recurrent hepatocellular carcinoma and its association with the expression of ZBP-89*, The American journal of pathology, 162(6), 1823–1829.

Chen, L., Zhang, W., Zhou, Q. D., Yang, H. Q., Liang, H. F., Zhang, B. X., Long, X., & Chen, X. P. (2012) *HSCs play a distinct role in different phases of oval cell-mediated liver regeneration*, Cell biochemistry and function, 30(7), 588–596.

Chen, Y. L., Lin, P. Y., Ming, Y. Z., Huang, W. C., Chen, R. F., Chen, P. M., & Chu, P. Y. (2017) *The effects of the location of cancer stem cell marker CD133 on the prognosis of hepatocellular carcinoma patients*, BMC cancer, 17(1), 474.

Cheng, A. L., Kang, Y. K., Chen, Z., Tsao, C. J., Qin, S., Kim, J. S., Luo, R., Feng, J., Ye, S., Yang, T. S., Xu, J., Sun, Y., Liang, H., Liu, J., Wang, J., Tak, W. Y., Pan, H., Burock, K., Zou, J., Voliotis, D., Guan, Z. (2009) *Efficacy and safety of sorafenib in patients in the Asia-Pacific region with advanced hepatocellular carcinoma: a phase III randomised, double-blind, placebo-controlled trial*, The Lancet. Oncology, 10(1), 25–34.

Chiba, T., Kanai, F., Iwama, A., & Yokosuka, O. (2013) *Circulating cancer stem cells: a novel prognostic predictor of hepatocellular carcinoma*, Hepatobiliary surgery and nutrition, 2(1), 4–6.

Cioffi, M., Dorado, J., Baeuerle, P. A., & Heeschen, C. (2012) *EpCAM/CD3-Bispecific T-cell engaging antibody MT110 eliminates primary human pancreatic cancer stem cells*, Clinical cancer research: an official journal of the American Association for Cancer Research, 18(2), 465–474.

Condeelis, J. and Pollard, J. W. (2006) *Macrophages: obligate partners for tumor cell migration, invasion, and metastasis*, Cell. Elsevier B.V., pp. 263–266.

Dudley, A. C. (2012) *Tumor endothelial cells*, Cold Spring Harbor Perspectives in Medicine, 2(3).

El-Khoueiry, A. B., Sangro, B., Yau, T., Crocenzi, T. S., Kudo, M., Hsu, C., Kim, T. Y., Choo, S. P., Trojan, J., Welling, T. H., Rd, Meyer, T., Kang, Y. K., Yeo, W., Chopra, A., Anderson, J., Dela Cruz, C., Lang, L., Neely, J., Tang, H., Dastani, H. B., Melero, I. (2017) *Nivolumab in patients with advanced hepatocellular carcinoma (CheckMate 040): an open-label, non-comparative, phase 1/2 dose escalation and expansion trial*, Lancet (London, England), 389(10088), 2492–2502.

Fan, S. T., Yang, Z. F., Ho, D. W., Ng, M. N., Yu, W. C., & Wong, J. (2011) *Prediction of posthepatectomy recurrence of hepatocellular carcinoma by circulating cancer*

stem cells: a prospective study, Annals of surgery, 254(4), 569–576.

Farazi, P. A. and Depinho, R. A. (2006) *Hepatocellular carcinoma pathogenesis: from genes to environment*, 6(September), pp. 674–687.

Finn, R. S. and Zhu, A. X. (2009) *Targeting angiogenesis in hepatocellular carcinoma: Focus on VEGF and bevacizumab*, Expert Review of Anticancer Therapy. Expert Rev Anticancer Ther, pp. 503–509.

Franco, O. E., Shaw, A. K., Strand, D. W., & Hayward, S. W. (2010) *Cancer associated fibroblasts in cancer pathogenesis*, Seminars in cell & developmental biology, 21(1), 33–39.

Franklin, R. A., Liao, W., Sarkar, A., Kim, M. V., Bivona, M. R., Liu, K., Pamer, E. G., & Li, M. O. (2014) *The cellular and molecular origin of tumor-associated macrophages*, Science (New York, N.Y.), 344(6186), 921–925.

Friedman, S. L. (2008) *Hepatic stellate cells: Protean, multifunctional, and enigmatic cells of the liver*, Physiological Reviews. Physiol Rev, pp. 125–172.

Galdiero, M. R., Bonavita, E., Barajon, I., Garlanda, C., Mantovani, A., & Jaillon, S. (2013) *Tumor associated macrophages and neutrophils in cancer*, Immunobiology, 218(11), 1402–1410.

Galdiero, M. R., Garlanda, C., Jaillon, S., Marone, G., & Mantovani, A. (2013) *Tumor associated macrophages and neutrophils in tumor progression*, Journal of cellular physiology, 228(7), 1404–1412.

Galon, J., Angell, H. K., Bedognetti, D., & Marincola, F. M. (2013) *The continuum of cancer immunosurveillance: prognostic, predictive, and mechanistic signatures*, Immunity, 39(1), 11–26.

Gao, B., Jeong, W. I., & Tian, Z. (2008) *Liver: An organ with predominant innate immunity*, Hepatology (Baltimore, Md.), 47(2), 729–736.

Gedaly, R., Galuppo, R., Daily, M. F., Shah, M., Maynard, E., Chen, C., Zhang, X., Esser, K. A., Cohen, D. A., Evers, B. M., Jiang, J., & Spear, B. T. (2014) *Targeting the Wnt/β-catenin signaling pathway in liver cancer stem cells and hepatocellular carcinoma cell lines with FH535*, PloS one, 9(6), e99272.

Geerts, A. (2001) *History, heterogeneity, developmental biology, and functions of quiescent hepatic stellate cells*, Seminars in Liver Disease, 21(3), pp. 311–335.

Glumac, P. M. and LeBeau, A. M. (2018) *The role of CD133 in cancer: a concise review*, Clinical and Translational Medicine, 7(1).

Gong, J., Chehrazi-Raffle, A., Reddi, S., & Salgia, R. (2018) *Development of PD-1*

and PD-L1 inhibitors as a form of cancer immunotherapy: a comprehensive review of registration trials and future considerations, Journal for immunotherapy of cancer, 6(1), 8.

Güler, G., Guven, U. and Oktem, G. (2019) *Characterization of CD133+/CD44+ human prostate cancer stem cells with ATR-FTIR spectroscopy*, Analyst, 144(6), pp. 2138–2149.

Guo, W., Lasky, J. L. and Wu, H. (2006) *Cancer stem cells*, Pediatric Research. Nature Publishing Group, pp. 59–64.

Hemmings, B. A., & Restuccia, D. F. (2012) *PI3K-PKB/Akt pathway*, Cold Spring Harbor perspectives in biology, 4(9), a011189.

Hermann, P. C., Huber, S. L., Herrler, T., Aicher, A., Ellwart, J. W., Guba, M., Bruns, C. J., & Heeschen, C. (2007) *Distinct populations of cancer stem cells determine tumor growth and metastatic activity in human pancreatic cancer*, Cell stem cell, 1(3), 313–323.

Ishibashi, H., Nakamura, M., Komori, A., Migita, K., & Shimoda, S. (2009) *Liver architecture, cell function, and disease*, Seminars in immunopathology, 31(3), 399–409.

Jain, R. K. (2009) *A New Target for Tumor Therapy*, New England Journal of Medicine, 360(25), pp. 2669–2671.

Ji, J. and Wang, X. W. (2012) *Clinical implications of cancer stem cell biology in hepatocellular carcinoma*, in Seminars in Oncology. W.B. Saunders, pp. 461–472.

Karagonlar, Z. F., Akbari, S., Karabicici, M., Sahin, E., Avci, S. T., Ersoy, N., Ates, K. E., Balli, T., Karacicek, B., Kaplan, K. N., Celiker, C., Atabey, N., & Erdal, E. (2020) *A Novel Function for KLF4 in Modulating the De-differentiation of EpCAM-/CD133- nonStem Cells into EpCAM+/CD133+ Liver Cancer Stem Cells in HCC Cell Line HuH7*, Cells, 9(5), 1198.

Keane, M. P., Strieter, R. M. and Belperio, J. A. (2005) *Mechanisms and mediators of pulmonary fibrosis*, Critical Reviews in Immunology. Crit Rev Immunol, pp. 429–463.

Khaitan, D., Chandna, S., Arya, M. B., & Dwarakanath, B. S. (2006) *Establishment and characterization of multicellular spheroids from a human glioma cell line; Implications for tumor therapy*, Journal of translational medicine, 4, 12.

Kuperwasser, C., Chavarria, T., Wu, M., Magrane, G., Gray, J. W., Carey, L., Richardson, A., & Weinberg, R. A. (2004) *Reconstruction of functionally normal and malignant human breast tissues in mice*, Proceedings of the National Academy of

Sciences of the United States of America, 101(14), 4966–4971.

Lee, U. E., Mstp, B. S. and Friedman, S. L. (2011) *Best practice & research clinical gastroenterology mechanisms of hepatic fibrogenesis*, Best Practice & Research Clinical Gastroenterology, 25(2), pp. 195–206.

Lee, J., Cuddihy, M. J., & Kotov, N. A. (2008) *Three-dimensional cell culture matrices: state of the art. Tissue engineering*, Part B, Reviews, 14(1), 61–86.

Li, C., Heidt, D. G., Dalerba, P., Burant, C. F., Zhang, L., Adsay, V., Wicha, M., Clarke, M. F., & Simeone, D. M. (2007) *Identification of pancreatic cancer stem cell,* Cancer research, 67(3), 1030–1037

Li, L., Zhao, G. D., Shi, Z., Qi, L. L., Zhou, L. Y., & Fu, Z. X. (2016) *The Ras/Raf/MEK/ERK signaling pathway and its role in the occurrence and development of HCC,* Oncology letters, 12(5), 3045–3050.

Lin, Z. Y., Chuang, Y. H. and Chuang, W. L. (2012) *Cancer-associated fibroblasts up-regulate CCL2, CCL26, IL6 and LOXL2 genes related to promotion of cancer progression in hepatocellular carcinoma cells*, Biomedicine and Pharmacotherapy, 66(7), pp. 525–529.

Llovet, J. M., Ricci, S., Mazzaferro, V., Hilgard, P., Gane, E., Blanc, J. F., de Oliveira, A. C., Santoro, A., Raoul, J. L., Forner, A., Schwartz, M., Porta, C., Zeuzem, S., Bolondi, L., Greten, T. F., Galle, P. R., Seitz, J. F., Borbath, I., Häussinger, D., Giannaris, T., SHARP Investigators Study Group (2008) *Sorafenib in advanced hepatocellular carcinoma*, The New England journal of medicine, 359(4), 378–390.

Llovet, J. M., Zucman-Rossi, J., Pikarsky, E., Sangro, B., Schwartz, M., Sherman, M., & Gores, G. (2016) *Hepatocellular carcinoma*, Nature reviews. Disease primers, 2, 16018.

Liu, J., Chen, S., Wang, W., Ning, B. F., Chen, F., Shen, W., Ding, J., Chen, W., Xie, W. F., & Zhang, X. (2016*) Cancer-associated fibroblasts promote hepatocellular carcinoma metastasis through chemokine-activated hedgehog and TGF-β pathways,* Cancer letters, 379(1), 49–59.

Liu, Y. (2006) *Renal fibrosis: New insights into the pathogenesis and therapeutics*, Kidney International. Kidney Int, pp. 213–217.

Liu, Y. C., Yeh, C. T. and Lin, K. H. (2020) *Cancer Stem Cell Functions in Hepatocellular Carcinoma and Comprehensive Therapeutic Strategies*, Cells, 9(6).

Ma, S., Chan, K. W., Hu, L., Lee, T. K., Wo, J. Y., Ng, I. O., Zheng, B. J., & Guan, X. Y. (2007) *Identification and characterization of tumorigenic liver cancer*

stem/progenitor cells, Gastroenterology, 132(7), 2542–2556.

Macdonald, B. T., Tamai, K. and He, X. (2009) *Review Wnt / b -catenin signaling : components , mechanisms , and diseases*, Developmental Cell, 17(1), pp. 9–26.

Maugeri-Saccà, M., Vigneri, P. and De Maria, R. (2011) *Cancer stem cells and chemosensitivity*, Clinical Cancer Research. American Association for Cancer Research, pp. 4942–4947.

Mazzocca, A., Dituri, F., Lupo, L., Quaranta, M., Antonaci, S., & Giannelli, G. (2011) *Tumor-secreted lysophostatidic acid accelerates hepatocellular carcinoma progression by promoting differentiation of peritumoral fibroblasts in myofibroblasts*, Hepatology (Baltimore, Md.), 54(3), 920–930.

McNamara, M. G., Le, L. W., Horgan, A. M., Aspinall, A., Burak, K. W., Dhani, N., Chen, E., Sinaei, M., Lo, G., Kim, T. K., Rogalla, P., Bathe, O. F., & Knox, J. J. (2015) *A phase II trial of second-line axitinib following prior antiangiogenic therapy in advanced hepatocellular carcinoma*, Cancer, 121(10), 1620–1627.

Meindl-Beinker, N. M., Matsuzaki, K., & Dooley, S. (2012) *TGF-β signaling in onset and progression of hepatocellular carcinoma*, Digestive diseases (Basel, Switzerland), 30(5), 514–523.

De Mingo Pulido, A. and Ruffell, B. (2016) *Immune regulation of the metastatic process: implications for therapy*, in Advances in Cancer Research. Academic Press Inc., pp. 139–163.

Moens, S., Goveia, J., Stapor, P. C., Cantelmo, A. R., & Carmeliet, P. (2014) *The multifaceted activity of VEGF in angiogenesis - Implications for therapy responses*, Cytokine & growth factor reviews, 25(4), 473–482.

Mohammed, M. K., Shao, C., Wang, J., Wei, Q., Wang, X., Collier, Z., Tang, S., Liu, H., Zhang, F., Huang, J., Guo, D., Lu, M., Liu, F., Liu, J., Ma, C., Shi, L. L., Athiviraham, A., He, T. C., & Lee, M. J. (2016) *Wnt/β-catenin signaling plays an ever-expanding role in stem cell self-renewal, tumorigenesis and cancer chemoresistance*, Genes & diseases, 3(1), 11–40.

O'Brien, C. A., Pollett, A., Gallinger, S., & Dick, J. E. (2007) *A human colon cancer cell capable of initiating tumour growth in immunodeficient mice*, Nature, 445(7123), 106–110.

Peng, L., Fu, J., Wang, W., Hofman, F. M., Chen, T. C., & Chen, L. (2019) *Distribution of cancer stem cells in two human brain gliomas*, Oncology letters, 17(2), 2123–2130.

Philip, P. A., Mooney, M., Jaffe, D., Eckhardt, G., Moore, M., Meropol, N., Emens, L., O'Reilly, E., Korc, M., Ellis, L., Benedetti, J., Rothenberg, M., Willett, C., Tempero, M., Lowy, A., Abbruzzese, J., Simeone, D., Hingorani, S., Berlin, J., & Tepper, J. (2009) *Consensus report of the national cancer institute clinical trials planning meeting on pancreas cancer treatment*, Journal of clinical oncology: official journal of the American Society of Clinical Oncology, 27(33), 5660–5669.

Piao, L. S., Hur, W., Kim, T. K., Hong, S. W., Kim, S. W., Choi, J. E., Sung, P. S., Song, M. J., Lee, B. C., Hwang, D., & Yoon, S. K. (2012) *CD133+ liver cancer stem cells modulate radioresistance in human hepatocellular carcinoma*, Cancer letters, 315(2), 129–137.

Prieto, J., Melero, I., & Sangro, B. (2015) *Immunological landscape and immunotherapy of hepatocellular carcinoma*, Nature reviews. Gastroenterology & hepatology, 12(12), 681–700.

Pruszak, J., Menon, V. and Pruszak, J. (2017) *The CD24 surface antigen in neural development and disease*, Neurobiology of Disease. Academic Press Inc., pp. 133–144.

Qiu, Q., Hernandez, J. C., Dean, A. M., Rao, P. H., & Darlington, G. J. (2011) *CD24-positive cells from normal adult mouse liver are hepatocyte progenitor cells*, Stem cells and development, 20(12), 2177–2188.

Racanelli, V., & Rehermann, B. (2006) *The liver as an immunological organ*, Hepatology (Baltimore, Md.), 43(2 Suppl 1), S54–S62.

Raoul, J. L., Frenel, J. S., Raimbourg, J., & Gilabert, M. (2019) *Current options and future possibilities for the systemic treatment of hepatocellular carcinoma*, Hepatic oncology, 6(1), HEP11.

Sancho-Bru, P., Juez, E., Moreno, M., Khurdayan, V., Morales-Ruiz, M., Colmenero, J., Arroyo, V., Brenner, D. A., Ginès, P., & Bataller, R. (2010) *Hepatocarcinoma cells stimulate the growth, migration and expression of pro-angiogenic genes in human hepatic stellate cells*, Liver international: official journal of the International Association for the Study of the Liver, 30(1), 31–41.

Sangro, B., Gomez-Martin, C., de la Mata, M., Iñarrairaegui, M., Garralda, E., Barrera, P., Riezu-Boj, J. I., Larrea, E., Alfaro, C., Sarobe, P., Lasarte, J. J., Pérez-Gracia, J. L., Melero, I., & Prieto, J. (2013) *A clinical trial of CTLA-4 blockade with tremelimumab in patients with hepatocellular carcinoma and chronic hepatitis C*, Journal of hepatology, 59(1), 81–88.

Senkowski, W., Jarvius, M., Rubin, J., Lengqvist, J., Gustafsson, M. G., Nygren, P., Kultima, K., Larsson, R., & Fryknäs, M. (2016) *Large-Scale Gene Expression Profiling Platform for Identification of Context-Dependent Drug Responses in Multicellular Tumor Spheroids*, Cell chemical biology, 23(11), 1428–1438.

Serova, M., Tijeras-Raballand, A., Dos Santos, C., Albuquerque, M., Paradis, V., Neuzillet, C., Benhadji, K. A., Raymond, E., Faivre, S., & de Gramont, A. (2015) *Effects of TGF-beta signalling inhibition with galunisertib (LY2157299) in hepatocellular carcinoma models and in ex vivo whole tumor tissue samples from patients*, *Oncotarget*, *6*(25), 21614–21627.

Sokolović, A., Sokolović, M., Boers, W., Elferink, R. P., & Bosma, P. J. (2010) *Insulin-like growth factor binding protein 5 enhances survival of LX2 human hepatic stellate cells*, Fibrogenesis & tissue repair, 3, 3.

Tsuyada, A., Chow, A., Wu, J., Somlo, G., Chu, P., Loera, S., Luu, T., Li, A. X., Wu, X., Ye, W., Chen, S., Zhou, W., Yu, Y., Wang, Y. Z., Ren, X., Li, H., Scherle, P., Kuroki, Y., & Wang, S. E. (2012) *CCL2 mediates cross-talk between cancer cells and stromal fibroblasts that regulates breast cancer stem cells*, Cancer research, 72(11), 2768–2779.

Villanueva, A., Newell, P., Chiang, D. Y., Friedman, S. L., & Llovet, J. M. (2007) *Genomics and signaling pathways in hepatocellular carcinoma*, Seminars in liver disease, 27(1), 55–76.

Villanueva, A., Newell, P., Chiang, D. Y., Friedman, S. L., & Llovet, J. M. (2007) *Genomics and signaling pathways in hepatocellular carcinoma*, Seminars in liver disease, *27*(1), 55–76.

Wan, S., Zhao, E., Kryczek, I., Vatan, L., Sadovskaya, A., Ludema, G., Simeone, D. M., Zou, W., & Welling, T. H. (2014) *Tumor-associated macrophages produce interleukin 6 and signal via STAT3 to promote expansion of human hepatocellular carcinoma stem cells*, Gastroenterology, 147(6), 1393–1404.

Weiss, A., & Attisano, L. (2013) *The TGFbeta superfamily signaling pathway. Wiley interdisciplinary reviews*, Developmental biology, 2(1), 47–63.

Whittaker, S., Marais, R. and Zhu, A. X. (2010) *The role of signaling pathways in the development and treatment of hepatocellular carcinoma*, Oncogene, pp. 4989–5005.

Wong, M. M., Chan, H. Y., Aziz, N. A., Ramasamy, T. S., Bong, J. J., Ch'ng, E. S., Armon, S., Peh, S. C., & Teow, S. Y. (2021) *Interplay of autophagy and cancer stem cells in hepatocellular carcinoma*, Molecular biology reports, 48(4), 3695–3717.

Xin, H. W., Ambe, C. M., Hari, D. M., Wiegand, G. W., Miller, T. C., Chen, J. Q., Anderson, A. J., Ray, S., Mullinax, J. E., Koizumi, T., Langan, R. C., Burka, D., Herrmann, M. A., Goldsmith, P. K., Stojadinovic, A., Rudloff, U., Thorgeirsson, S. S., & Avital, I. (2013) *Label-retaining liver cancer cells are relatively resistant to sorafenib*, Gut, 62(12), 1777–1786.

Yamada, K. M. and Cukierman, E. (2007) *Modeling Tissue Morphogenesis and Cancer in 3D*, Cell. Elsevier B.V., pp. 601–610.

Yamashita, T., Ji, J., Budhu, A., Forgues, M., Yang, W., Wang, H. Y., Jia, H., Ye, Q., Qin, L. X., Wauthier, E., Reid, L. M., Minato, H., Honda, M., Kaneko, S., Tang, Z. Y., & Wang, X. W. (2009) *EpCAM-positive hepatocellular carcinoma cells are tumor-initiating cells with stem/progenitor cell features. Gastroenterology*, 136(3), 1012–1024.

Yang, W., Yan, H. X., Chen, L., Liu, Q., He, Y. Q., Yu, L. X., Zhang, S. H., Huang, D. D., Tang, L., Kong, X. N., Chen, C., Liu, S. Q., Wu, M. C., & Wang, H. Y. (2008) *Wnt/beta-catenin signaling contributes to activation of normal and tumorigenic liver progenitor cells*, Cancer research, 68(11), 4287–4295.

Zhu, A. X., Finn, R. S., Edeline, J., Cattan, S., Ogasawara, S., Palmer, D., Verslype, C., Zagonel, V., Fartoux, L., Vogel, A., Sarker, D., Verset, G., Chan, S. L., Knox, J., Daniele, B., Webber, A. L., Ebbinghaus, S. W., Ma, J., Siegel, A. B., Cheng, A. L., KEYNOTE-224 investigators (2018) *Pembrolizumab in patients with advanced hepatocellular carcinoma previously treated with sorafenib (KEYNOTE-224): a non-randomised, open-label phase 2 trial*, The Lancet. Oncology, 19(7), 940–952.

Zhu, A. X., Rosmorduc, O., Evans, T. R., Ross, P. J., Santoro, A., Carrilho, F. J., Bruix, J., Qin, S., Thuluvath, P. J., Llovet, J. M., Leberre, M. A., Jensen, M., Meinhardt, G., & Kang, Y. K. (2015) *SEARCH: a phase III, randomized, double-blind, placebo-controlled trial of sorafenib plus erlotinib in patients with advanced hepatocellular carcinoma*, Journal of clinical oncology: official journal of the American Society of Clinical Oncology, 33(6), 559–566.